Check for updates

Immune-enhancing effect of *Weizmannia coagulans* BCG44 and its supernatant on cyclophosphamide-induced immunosuppressed mice and RAW264.7 cells *via* the modulation of the gut microbiota†

Yafang Xu,‡[a] Yi Wang,‡[b] Tao Song,‡[c] Xiaxia Li,[a] Haolin Zhou,[a] Oumarou Zafir Chaibou,[a] Bing Wang[b] and Huajun Li ⓘ *[a]

We established a model of cyclophosphamide (CTX)-induced immunosuppressed mice and RAW264.7 cells to assess the effectiveness of *W. coagulans* BCG44 and its supernatant in enhancing immune function and modulating the gut microbiota. *W. coagulans* BCG44 and its supernatant restored Th17/Treg balance and alleviated gut inflammation by elevating the expression of interleukin-10 (IL-10) and decreasing IL-6 and toll-like receptor 4 (TLR4). Meanwhile, *W. coagulans* BCG44 and its supernatant downregulated the levels of lipopolysaccharide and D-lactic acid while increasing the expression of tight junction proteins (ZO-1 and occludin) and goblet cells/crypts to ameliorate mucosal damage. *W. coagulans* BCG44 and its supernatant may restore the gut microbiota in the immunosuppressed mice by regulating keystone species (*Lactobacillus* and *Lachnospiraceae*). PICRUSt2 function prediction and BugBase analysis showed that *W. coagulans* BCG44 and its supernatant significantly down-regulated American trypanosomiasis and potentially_pathogenic. In addition, under normal *versus* inflamed culture conditions, stimulation of RAW246.7 cells with *W. coagulans* BCG44 supernatant activated immune response with increasing proliferation ability and the gene expression of IL-10 while decreasing TLR4. Metabolites in the *W. coagulans* BCG44 supernatant included arginine, tyrosine, solamargine, tryptophan, D-mannose, phenyllactic acid, and arachidonic acid. Collectively, these findings suggested that *W. coagulans* BCG44 and its supernatant possess potential immunomodulatory activity and modulate gut microbiota dysbiosis in the CTX-induced immunosuppressed mice.

Introduction

The regulation of immune responses plays a critical role in disease prevention and treatment. Besides its absorptive function, the healthy mucosal barrier acts as a protective shield against pathogenic microorganisms and toxins by effectively regulating immune responses.[1] The diversity of the gut microbiota is closely linked to intestinal mucosal immunity as it produces both pro-inflammatory and anti-inflammatory responses that facilitate self-regulation of intestinal microbial ecology.[2] However, dysfunction of the immune system often coincides with dysregulation of the gut microbiota, which may contribute to various diseases.[2] Cyclophosphamide (CTX) is extensively utilized as a chemotherapeutic agent in the treatment of cancer, making it one of the most prevalent anti-neoplastic drugs.[3] It is particularly toxic to immunocompetent cells *via* impaired T-cell responses, such as helper T cells 17 (Th17) and regulatory T lymphocytes (Treg),[4] and thereby increases the suppression of patients' immune systems.[5] The proinflammatory cytokine interleukin-17 (IL-17) is secreted by Th17 cells in response to stimulation by IL-6, whereas Treg exerts opposite effects by actively inhibiting the activation of potentially autoreactive T cells under normal conditions.[6] Long-term use of CTX can lead to dysbiosis in intestinal flora and disruption of the intestinal barrier, resulting in intestinal leakage.[7]

Immune regulation and stimulation induced by probiotics and their metabolites have garnered increasing attention. Administering probiotics and their metabolites can modulate

[a]*Department of Pathogen Biology and Microecology, College of Basic Medical Sciences, Dalian Medical University, Dalian, China. E-mail: lhjcmu@hotmail.com; Fax: +86 0411 86110282; Tel: +86 0411 86110305*
[b]*Department of Immunology, College of Basic Medical Sciences, Dalian Medical University, Dalian, China*
[c]*Department of Biotechnology, College of Basic Medical Sciences, Dalian Medical University, Dalian, China*
†Electronic supplementary information (ESI) available. See DOI: https://doi.org/10.1039/d4fo02452d
‡These authors contributed equally to this work.

the composition and functionality of the gut microbiota, enhance the integrity and function of the intestinal epithelial barrier, and augment the host's immune response within the gastrointestinal tract.[8,9] *Weizmannia coagulans*, (known as *Bacillus coagulans*, *B. coagulans*), as a lactic acid-producing, spore-forming bacterial species, has significant probiotic effects on regulating the body's intestines and immunity.[10,11] *B. coagulans* consumes free oxygen in the digestive tract, leading to the formation of an anaerobic and acidic digestive environment. This environment inhibits the growth of pathogenic bacteria and provides a more favorable growth environment for beneficial bacteria such as *Lactobacillus*.[4,12] Zhao *et al.* discovered that *B. coagulans* 13 002 enhanced the abundance of *Bifidobacteria* and *Lactobacillus*, thereby modulating immune responses triggered by CTX.[13] *B. coagulans* MZY531 exhibited anti-inflammatory properties by enhancing the production of mucin, which facilitated the adherence of beneficial bacteria while preventing the attachment of pathogens.[14] Crucially, the metabolites secreted by *B. coagulans* exert diverse advantageous effects on the host.[15] These include increased production of mucin and tight junction proteins, which help maintain the integrity of the epithelial barrier,[16] and antimicrobial peptides (such as bacteriocins),[17] which can prevent pathogenic biofilm formation. Additionally, macrophages are not only essential antigen-presenting cells, but also an important link connecting innate and adaptive immunity.[18] These metabolites derived from *B. coagulans* elicit immune responses by augmenting macrophage activity and modulating immunoglobulin secretion.[19]

Nevertheless, the effects of the supernatant of *W. coagulans* on immunity and gut microbiota remain unclear. Therefore, this study investigated the immunomodulatory effect and regulation of gut microbiota by *W. coagulans* BCG44 and its supernatant in a CTX-induced immunosuppressed mice model. The study also investigated the immune mechanism in activating RAW264.7 cells and the bioactive metabolites in the *W. coagulans* BCG44 supernatant.

Materials and methods

Preparation of bacterial strains and reagent

W. coagulans BCG44 was obtained from BioGrowing Co., Ltd (Shanghai, China). Each gram of powder contains 2×10^{10} colony-forming units (CFU) of *W. coagulans* BCG44. Cyclophosphamide (CTX) was purchased from Jiangsu Hengrui Medicine Co., Ltd (Jiangsu, China).

Bacterial culture and preparation of the cell-free supernatant

W. coagulans BCG44 was activated three times by aseptic inoculation (2% v/v) in Man-Rogosa-Sharpe (MRS) broth (peptone 10.0 g, beef extract 10.0 g, glucose 20.0 g, yeast extract powder 5.0 g, sodium acetate 5.0 g, dipotassium hydrogen phosphate 2.0 g, tri-ammonium citrate 2.0 g, magnesium sulfate 0.5 g, manganese sulfate 0.05 g, Tween-80 1.0 g, distilled water 1000 mL, pH 6.5, autoclaved for 15 min at 121 °C),[20] and the

facultative anaerobes were incubated at 37 °C for 16–18 h (ref. 21) (ESI Fig. 1†). The supernatant was prepared *via* centrifugation at 6000 rpm for 10 minutes at 4 °C, and dual filtration through 0.22 μm Millipore filters.[22]

Animal and experimental design

Thirty-two male BALB/c mice, 6–7 weeks old (22 ± 2 g), were purchased from Dalian Medical University (Animal permission number: SCXK-20220-0001). The specific-pathogen-free grade mice were placed in a normal environment room under constant temperature (22 ± 2 °C) and humidity ($50 \pm 10\%$), and adapted for a week with a light/dark cycle of 12 h (Model Animal Research Centre, Dalian Medical University, China). All animal procedures were performed in accordance with the Ethical Guidelines for the Care and Use of Laboratory Animals of Dalian Medical University, and approved by the Animal Ethics Committee of Dalian Medical University (AEE23075). As shown in Fig. 1a, the experimental mice were randomly divided into four groups: the normal group (N, $n = 8$), the model group (M, $n = 8$), the *W. coagulans* BCG44 group (BC, $n = 8$), and the *W. coagulans* BCG44 supernatant group (BCS, $n = 8$). During the whole experiment, N and M groups were respectively gavaged with 0.2 mL day^{-1} normal saline. The BC group was gavaged with 2×10^6 CFU mL^{-1} day^{-1} of *W. coagulans* BCG44 per mouse,[23] and the BCS group was administered at 0.2 mL day^{-1} supernatant by gavage. In the last four (from day 24 to day 28) days, the M, BC, and BCS groups received intraperitoneal administration of CTX at a dose of 60 mg kg^{-1} (Jiangsu Hengrui Medicine Co., Ltd, China) once a day, and the N group was administered an equivalent volume of saline. The mice were euthanized by carbon dioxide asphyxiation on the 28th day of the experiment, and immune cells from the spleen were subsequently isolated. Meanwhile, the spleen, distal ileum (1 cm proximal to the caecum)[24] and proximal colon tissues[25] were formalin-fixed overnight at room temperature, and then embedded in paraffin. The 10 cm distal ileum[24] and cecal contents were rapidly frozen in liquid nitrogen, and stored at −80 °C for subsequent analysis.

Body weight and immune organ index

The weight of each mouse was recorded once every 7 days. During the autopsy, the spleen was weighed and the spleen index was calculated. The visceral index was calculated as follows: Spleen index (mg g^{-1}) = Spleen weight/body weight.

Measurement of inflammatory cytokine and intestinal permeability

According to the previous experimental method,[26] serum was collected from blood samples through centrifugation at 3000 rpm and 4 °C for 15 minutes. The serum tumor necrosis factor-α (TNF-α), D-lactic acid (D-LA) and lipopolysaccharide (LPS) levels were measured at the corresponding absorbance using enzyme-linked immunosorbent assay (ELISA) kits (Jiangsu Mei Biao Bio-Technology Co., Ltd, China).
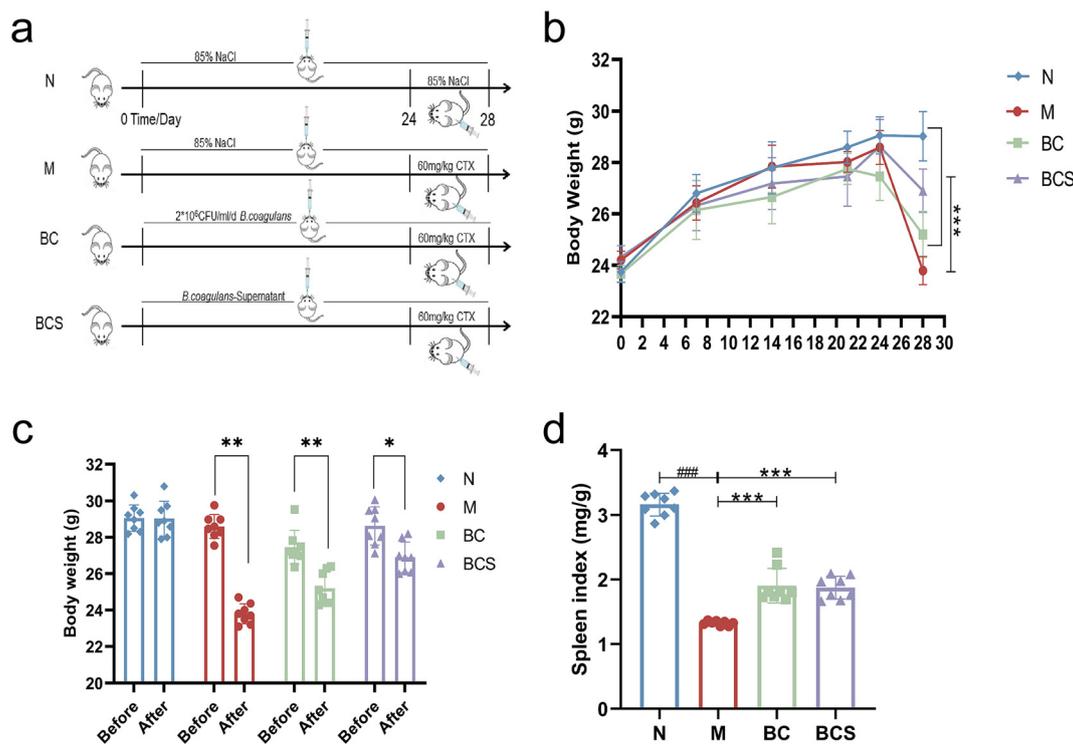
Fig. 1 Evaluation of *W. coagulans* BCG44 and its supernatant in the CTX-induced immunosuppressed mice model. (a) Animal and experimental design, and (b) body weight change. (c) The body weight was recorded before and after the injection of cyclophosphamide. (d) Spleen index.

Flow cytometry of lymphocyte subpopulations

Following our previously reported experimental protocol,[26] mouse spleens were triturated to obtain a spleen cell suspension at a concentration of 1×10^6 cells per mL. All of the antibodies were used at a dilution of 1 : 100. The cells were incubated with antibodies for 30 minutes at a temperature of 4 °C for cell surface staining AF488-CD4 (eBioscience, USA). The Foxp3 Fix/Perm kit (eBioscience) was used for intracellular transcription factor: PE-Foxp3 (eBioscience, USA) staining according to the manufacturer's instructions. For cytokine staining, cells were restimulated with 20 nM phorbol 12-myristate 13-acetate, 1.3 μM ionomycin and brefeldin A solution (Fcmacs Biotech Co., Ltd, Nanjin, China) in RPMI 1640 medium (Corning) supplemented with 10% FBS and penicillin–streptomycin for 4 h. Intracellular staining for the indicated cytokines APC-IL-17A (17-7177-81, eBioscience) was fixed using the Cytofix/Cytoperm kit (BD Biosciences), according to the manufacturer's instructions. Flow cytometry (Cyto Flex, Beckman Coulter, Inc. Brea, CA, U.S.A) was used to detect the cell phenotype for analysis.

Histopathological staining of the spleen, ileum and colon intestinal tissues

The paraffin-embedded spleen, ileum, and colon tissues (5 μm-thick sections) were prepared for HE staining, Alcian blue periodic acid Schiff staining, and immunofluorescence.[26,27] Referring to the following criteria,

the pathological severity of the spleen (400×, $n = 5$ per group) was blindly scored by two pathologists, as follows: 0 point: normal; 1 piont, necrosis of the follicle center; 2 points, blood sinus dilation or arteriolar sclerosis; 3 points, necrosis of the follicular center, blood sinus dilatation and arteriolar sclerosis.[28,29] For the ileum tissues, the intestinal villus length and crypt depth were determined by measuring at least 20 well-oriented, intact villus-crypt structures using Image Pro Plus 6.0 software (Media Cybernetics, MD, USA).[30–32] The length of each villus was measured from the top of the villus to the crypt transition, and the definition of the crypt depth was the invaginated depth between adjacent villi.[33] Based on the previously described scoring system,[34] colon tissues ($n = 5$ per group) were graded blindly for the severity of tissue damage at regions by two pathologists. The histopathology score is as follows: inflammation distribution (grade 0–3), crypt distortion and ulceration (grade 0–5), tissue damage (grade 0–3), inflammatory infiltration (grade 0–3), goblet cell loss (grade 0–3), and mucosal thickening (edema) (grade 0–3).[34] An optical microscope (Nikon Instruments Co., Ltd, Japan) was used to take images at 100× and 400× magnifications (Nikon Instruments Co., Ltd, Japan).

Alcian blue periodic acid Schiff staining (AB-PAS)

Following our previously reported experimental protocol,[27] paraffin sections of colon tissues were prepared for AB-PAS. Generally speaking, the assessment of mucous cell numbers in each recess can be utilized to estimate the proportion of goblet

cells that completely expel the intracellular mucus. The 15 to 30 crypts were examined on each slide, and 500 to 1000 stained mucus cells were quantified per colon sample ($n = 3$ per group). A recess is considered when it is cut along or near at least two-thirds of its length. All stained mucus cells from the bottom to the opening of both sides of the glandular cavity are included in the count, encompassing goblet cells with diffuse AB-PAS positive mucus particles, as well as those without obvious AB-PAS positive mucus particles. Mucous particles are excluded from counting. All slides were analyzed by a researcher who was unaware of the drug therapy.[35]

Immunofluorescence

The paraffin-embedded ileum tissue was heated in 1× EDTA Antigen Retrieval Solution (pH 8.0) for antigen retrieval after being pretreated with 3% H_2O_2 and 0.3% TritonX-100 for 15 min at room temperature. After blocking for 1 h, the samples were incubated overnight at 4 °C with a 1 : 200 dilution of anti-secretory occludin and anti-zonule occludin-1 (ZO-1) rabbit antibodies (Bioss, Beijing, China). After being washed with PBS, the sections were incubated with a mixture of Alexa CoraLite488-conjugated Goat Anti-Mouse IgG (H + L) (1 : 500; Proteintech, Wuhan, China) and CoraLite594-conjugated Goat Anti-Rabbit IgG (H + L) (1 : 300; Proteintech, Wuhan, China) secondary antibodies for 1 h at room temperature. All of the sections were counterstained with DAPI (1 : 10 000, Beyotime Biotechnology, Shanghai, China). Images were obtained using the confocal microscope ZEISS LSM 900 for materials (Carl Zeiss Microscopy GmbH, Jena, Germany) The integrated optical density of occludin and ZO-1 in the ileum mucosa was determined using the Image J analysis system (Media Cybernetics, Inc.). The immunostaining quantification reflects the expression of occludin and ZO-1.[36]

RNA extraction and quantitative real-time PCR

The 10 cm distal ileum tissue[24] (100 mg per sample) was used for RNA extraction and cDNA synthesis using SevenFast® Total RNA Extraction Kit (Beijing Seven Innovation Biotechnology Co., Ltd, Beijing, China). For qRT-PCR, 500 ng of cDNA was used for amplification, which was conducted with 2× SYBR Green Pro Taq HS Premix (Accurate Biology Co., Ltd, Hunan, China) on the LineGene 9600 plus with fluorescence quantitative polymerase chain reaction (Hangzhou Bioer Technology Co., Ltd, Hangzhou, China.). Various gene expressions were evaluated, including IL-6, IL-10, TLR4, and tight junction-associated proteins (occludin and ZO-1). All primers were synthesized by Sangon Biotech Co., Ltd (Shanghai, China) and are listed in Table S1.† β-Actin was used as a reference gene to calculate the relative levels of target genes based on the $2^{-\Delta\Delta Ct}$ method.[26]

Gut microbiota DNA extraction and 16S rRNA gene high-throughput sequencing

Five cecal contents (per group) were randomly selected from each group, and the genomic DNA was extracted using the stool DNA isolation kit (Foregene, China). According to the previous study,[26,27] genomic DNA was amplified by using poly-merase chain reaction (PCR) with universal primers. The universal primers were 338F (5′-ACTCCTACGGGAGGCAGCAG-3′) and 806R (5′-GGACTACHVGGGTWTCTAAT-3′). The purified amplicons were combined in equimolar masses and sequenced on the Illumina MiSeq PE300 platform/NovaSeq PE250 platform (Illumina, San Diego, U.S.A.). The UPARSE software was used to perform ASV clustering of the V3–V4 hypervariable regions of the bacterial 16S rRNA gene sequences based on about 100% similarity, processing optimized data using sequence noise reduction methods (DADA2/Deblur, etc.). The microbial dysbiosis index (MDI),[37] alpha diversity (Chao, Ace, Sobs, Shannon, Simpson, and coverage index), and beta diversity of the samples were calculated using QIIME 2 analysis of the ASV level. Statistical analyses were performed, and bacterial abundance and diversity were calculated. To predict the abundances of functional pathways using KEGG, the gut microbiota was analyzed by PICRUSt 2.[27] At the same time, BugBase was adopted to forecast the bacterial composition based on sequencing results.[38]

In vitro raw 264.7 cell culture

Mouse mononuclear macrophage cells (RAW 264.7 cells) were cultured in Dulbecco's Modified Eagle's Medium (DMEM) (Procell Life Science & Technology Co., Ltd, Wuhan, China) supplemented with 10% heat-inactivated fetal bovine serum (FBS; Beijing Solarbio Science & Technology Co., Ltd, Beijing, China) and 1% penicillin mixture (MeilunBio, Dalian, China) at 37 °C under 5% CO_2 atmosphere. RAW 264.7 cells in the logarithmic growth phase were seeded in the 6-well plate or 96-well plate at a density of 1×10^5 cells per well, and intervened with 0, 4, 8, 16, and 32 μM CTX for 24 h, respectively. According to the CTX concentrations,[39] the optimal concentration of CTX (8 μM) was determined by observing the cell viability. Under the drug intervention of CTX, RAW 264.7 cells were co-cultured with the supernatant of W. coagulans BCG44 (diluted to a ratio of 1 : 80, 1 : 40 and 1 : 20; BCS group) for 24 hours to observe the cell viability and the gene expression levels of inflammatory factors (IL-6, IL-10 and TNF-α). Moreover, the supernatant (1 : 40) without the CTX intervention was used to observe cell proliferation at 0, 24 and 48 h. Inflammatory factor gene expression was performed by RT-qPCR (specific experimental steps are described in the part on RNA extraction and quantitative real-time PCR). Cell viability was determined by CCk8 assay, as follows: the RAW246.7 cell suspension (100 μL per well) was seeded in a 96-well culture plate, and stimulated with the corresponding drugs and supernatants under the standard culture conditions of 37 °C and 5% CO_2 for proliferation experiments. After the addition of 10 μL cell counting Kit (CCK-8) solution to each well and subsequent incubation for 1 h, the absorbance value at 450 nm was measured by enzyme-linked immunosorbent assay. The control group did not receive any intervention.

Metabolomics

Untargeted metabolomics in the bacterial supernatant were analyzed at Shanghai Personal Biotechnology Cp., Ltd using a

UHPLC (1290 Infinity LC, Agilent Technologies) coupled to a quadrupole time-of-flight MS (AB Sciex TripleTOF 6600). Bacterial supernatant was added with 500 mL extract of methanol–acetonitrile–water (2 : 2 : 1, vol/vol/vol), vortexed and centrifuged at 14 000g for 20 min, and analyzed using a 2.1 mm × 100 mm ACQUIY UPLC BEH 1.7 μm column (waters, Ireland) for HILIC separation. In both ESI positive and negative modes, the mobile phase contained A = 25 mM ammonium acetate and 25 mM ammonium hydroxide in water and B = acetonitrile. For specific metabolite of peak picking and comparison, the raw MS data (wiff. scan files) were converted to .mzXML files using ProteoWizard MS Convert, before being imported into freely available XCMS software.

Statistical analysis

Data were presented as the mean ± standard deviation (SD). All statistical analyses were performed using Graph Pad Prism Version 9.5 (Graph Pad Software Inc., U.S.A.) and OriginPro 2021 v9.8.0.200 (OriginLab Corporation, U.S.A.). Statistical analysis of the KEGG pathway data was performed with STAMP v2.1.3. Data were analyzed using one-way analysis of variance (ANOVA) and Duncan's multiple range tests. The Benjamini-Hochberg method was employed to correct the false discovery rate of P values. Statistical significance was established at $P <$ 0.05, which was considered statistically significant.[27] #$P <$ 0.05, ##$P <$ 0.01 and ###$P <$ 0.001 vs. the N group; *$P <$ 0.05, **$P <$ 0.01 and ***$P <$ 0.001 vs. the M group.

Result

W. coagulans BCG44 and its supernatant ameliorated the body weight and immune organ index in CTX-induced immunosuppressed mice

Recording the body weight and overall status of mice from day 1 to day 28 (Fig. 1b), mice injected intraperitoneally with CTX showed a linear decrease in body weight, accompanied by a decline in health status ($P <$ 0.05) (Fig. 1b and c). However, the body weight shift observed in the groups treated with BC and its supernatant BCS was significantly smaller than that of the M group ($P <$ 0.05) (Fig. 1c and ESI Video†). As an important indicator reflecting immune status, the spleen indexes of the M group significantly decreased by 58.12% in comparison to the N group, while the spleen indexes of the BC and BCS groups significantly increased by 43.74% and 41.51% ($P <$ 0.05), respectively (Fig. 1d, Fig. S2 and Table S2†).

W. coagulans BCG44 and its supernatant enhanced the immune response in CTX-induced immunosuppressed mice

According to the histological section of the spleen (Fig. 2a), compared with the N group, the M group showed spleen parenchyma that were disorderly arranged with unclear boundaries between the red pulp and white pulp, characterized by less and scattered white pulp and germinal center, evident spleen beam fracture in the red pulp, and an elevated deposition of hemosiderin ($P >$ 0.05). The pathological scores of the

spleen in the BC and BCS groups were significantly lower than those in the M group, showing that the splenic capsule was relatively intact, the white pulp atrophy was mitigated and closely arranged with the clear edges, and the deposition of hemosiderin was reduced ($P <$ 0.05).

We compared the CD4$^+$ IL-17A$^+$ Th17 cell population and CD4$^+$ Foxp3$^+$ Treg cell population in the spleen by flow cytometry (Fig. 2b–g). The population of CD4$^+$ T lymphocytes in the spleen was significantly elevated in the M group compared to the N group ($P <$ 0.05), while there was no significant decrease observed in the BC and BCS groups when compared to the M group (Fig. 2d). As shown in Fig. 2b–g, the percentage of Th17 cells in the M group was significantly increased compared to the N group ($P <$ 0.05), while it was downregulated in the BC and BCS groups. Conversely, the Treg cell levels exhibited an opposite trend ($P <$ 0.05). Furthermore, immunosuppressed mice induced by CTX demonstrated a significant increase in the Th17/Treg ratio (Fig. 2g) in the spleen. However, both the BC and BCS groups significantly downregulated this ratio ($P <$ 0.05).

W. coagulans BCG44 and its supernatant adjusted the serum and ileum levels of immune cytokines in CTX-induced immunosuppressed mice

As shown in Fig. 3, the serum TNF-α level of the M group was significantly higher than that of the N group ($P <$ 0.05). However, the BC and BCS groups both significantly reduced the expression of TNF-α ($P <$ 0.05). At the gene level, the mRNA relative expression levels of IL-6 and TLR4 genes in the M groups were significantly higher than those in the N group ($P <$ 0.001; Fig. 3d and e). Conversely, compared with the M group, the expression levels of IL-6 and TLR4 genes in the BC and BCS groups were significantly reduced ($P <$ 0.001; Fig. 3d and e). The relative expression of the IL-10 gene in the ileum of the M group was significantly reduced compared to the N group ($P <$ 0.01), but the relative mRNA expression of the IL-10 gene (Fig. 3f) was reversed after the intervention with *W. coagulans* and its supernatant ($P <$ 0.01).

W. coagulans BCG44 and its supernatant improved the intestinal barrier in CTX-induced immunosuppressed mice

As shown in Fig. 3a–e, the serum levels of D-LA and LPS were significantly elevated in the M group compared to the N group ($P <$ 0.05). However, compared to the M group, both BC and BCS groups exhibited significantly lower serum LPS levels ($P <$ 0.05), with the BCS group showing a notably lower serum D-LA level than the M group ($P <$ 0.05).

Visualization of ileum (Fig. 4a–c) and colon sections (Fig. S3a and b†) stained with H&E staining showed that the lamina propria was exposed to infiltration of inflammatory cells and locally slight edema, with shortening and shedding villi length and locally lacking the mucosal layer and intestinal epithelium upon histological examination of the ileum of the M group ($P <$ 0.05; Fig. 4a–c). In contrast, BC and BCS groups were alleviated with mucosal and intestinal villus damage and improved crypt structure ($P <$ 0.05; Fig. 4a–c). The same results were also found
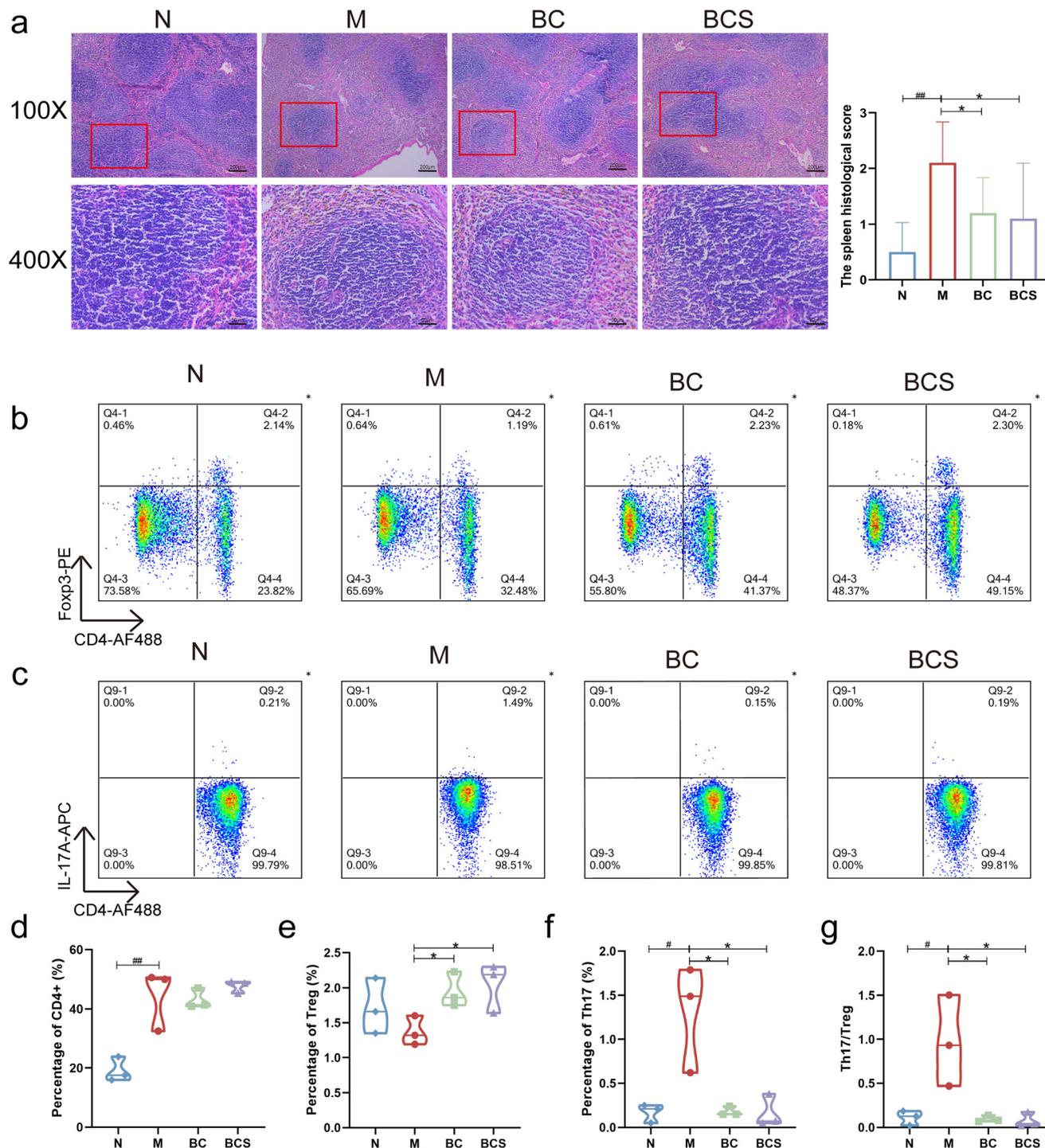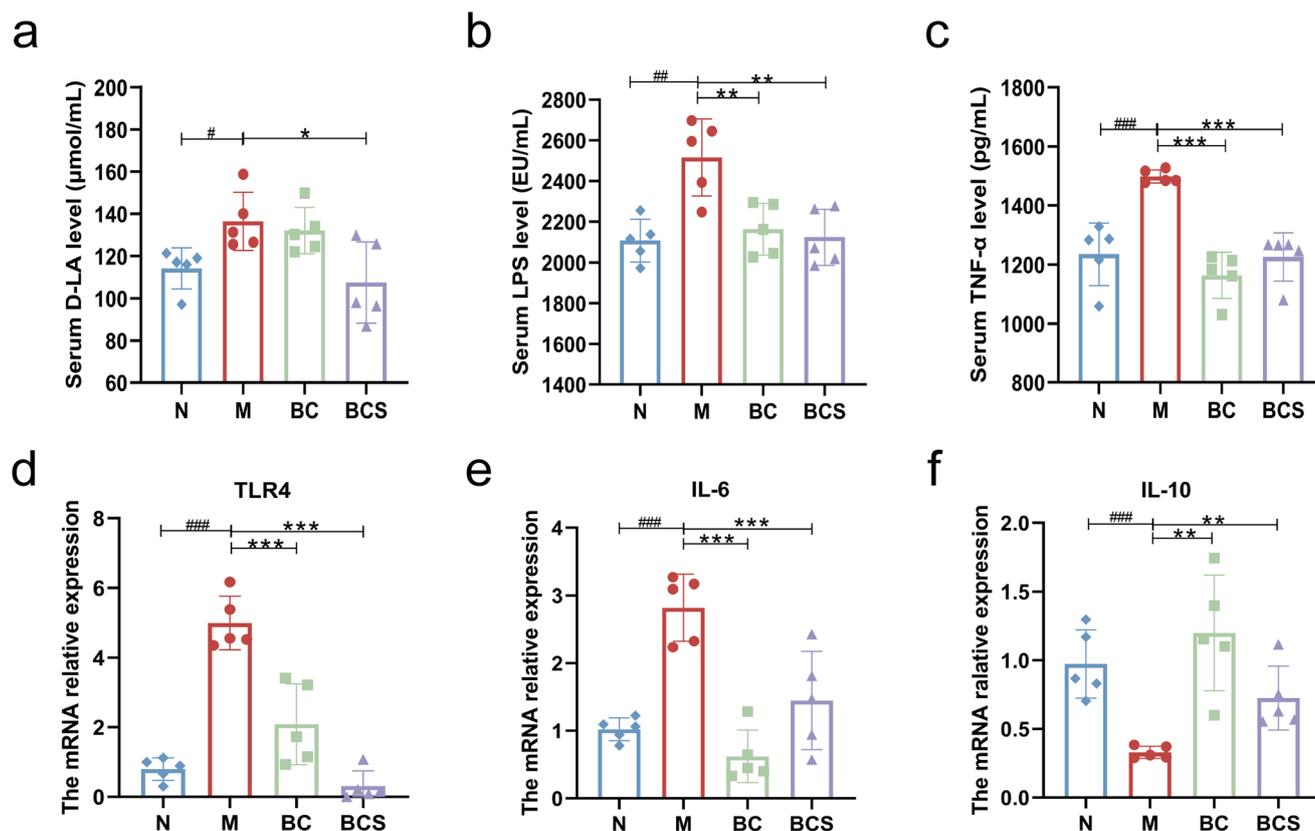
Fig. 2 Effect of *W. coagulans* BCG44 and its supernatant on immune function in CTX-induced immunosuppressed mice. (a) Representative images of the spleen samples stained by HE staining and the corresponding histological score (100× and 400× magnification, $n = 5$). (b) Frequencies of Th17 cells in the spleen. (c) Frequencies of Treg cells in the spleen. (d) The percentages of CD4$^+$ T cells (%), (e) Treg cells (%), (f) Th17 cells (%), and (g) Th17/Treg.

in colon HE staining with lower colonic histological scores of the BC and BCS groups ($P < 0.05$; Fig. S3a and b†).

We further analyzed the results of immunofluorescence staining and the relative gene expression levels of intestinal tight junc-

tion (TJ) proteins: zonula occludens protein-1 (ZO-1) and occludin in the ileum (Fig. 4d–h). Our results showed a significant reduction in both average fluorescence intensity and relative gene expression levels of ZO-1 and occludin in the M group

Fig. 3 Effects of *W. coagulans* BCG44 and its supernatant on the intestinal inflammation and endotoxemia induced by CTX. (a) Serum D-LA level (μmol mL^{-1}), (b) serum LPS level (EU mL^{-1}), (c) serum TNF-α level (pg mL^{-1}), and (d–f) the mRNA relative expression level of TLR4, IL-6 and IL-10 in the ileum as analysed using RT-qPCR.

compared to the N group ($P < 0.05$). However, both the BC and BCS groups significantly enhanced the expression of ZO-1 and occludin ($P < 0.05$) (Fig. 4d–h). Meanwhile, the AB-PAS staining was performed to assess colonic mucin production, which demonstrated a decrease in mucin production, along with a reduced number of goblet cells/Crypts in the M group compared to the N group ($P < 0.05$; Fig. S3c and d†). Remarkably, both BC and BCS groups exhibited an increased number of goblet cells/Crypts compared to the M group ($P < 0.05$) (Fig. S3c and d†).

W. coagulans BCG44 and its supernatant repaired gut microbiota dysbiosis in CTX-induced immunosuppressed mice

Using high-throughput sequencing of the V3 and V4 hypervariable regions of the 16S rRNA gene, we investigated the impact of *W. coagulans* and its supernatant on the gut microbiota in the CTX-induced immunosuppressed mice. The microbial dysbiosis index (MDI) at the Amplicon Sequence Variant (ASV) level (Fig. S5a†) was significantly higher in the M group, and the intervention groups were significantly increased compared to the N group ($P < 0.05$). The Shannon and Simpson indices characterize the community diversity; and the M group increased the Simpson index and decreased the Shannon index compared with those of the N group ($P < 0.05$) (Fig. S5b and c†). The Sobs, Chao, and ACE indices

showed similar results among the groups without significant differences (Table S3†). The gut microbiota structure using cecal samples was determined by principal coordinates analysis (PCoA), nonmetric dimensional scaling (NMDS) and the hierarchical clustering tree; these samples were separated into four clear clusters ($P < 0.05$) (Fig. 5d, e and Fig. S5e†). Four groups exhibited distinct microbial community characteristics, in which 467 ASVs existing in all groups were defined as core ASVs. The BC and BCS groups markedly increased the abundance of these ASVs (Fig. S5d†).

The specific changes in bacterial communities were investigated by cluster histograms to illustrate the alterations in intestinal microbiota at the phylum, family, and genus levels for each sample, as well as within subgroups (Fig. 5a–c). At the phylum level, *Firmicutes* and *Bacteroidetes* were dominant across all groups. The relative abundance of *Firmicutes* in both BC and BCS groups was significantly higher than that of the N group ($P < 0.05$). Additionally, the relative abundance of *Bacteroidota* in the BC and BCS groups decreased significantly compared to the M group ($P < 0.05$), whereas the relative abundance of *Actinbacterota* and *Desulfobacterota* showed no differences between the groups (Fig. 5a).

Furthermore, at the family level, compared with the N and M groups, the relative abundance of *Lactobacillaceae* and *Bacillaceae* both showed a significant increase ($P < 0.05$), whereas the relative
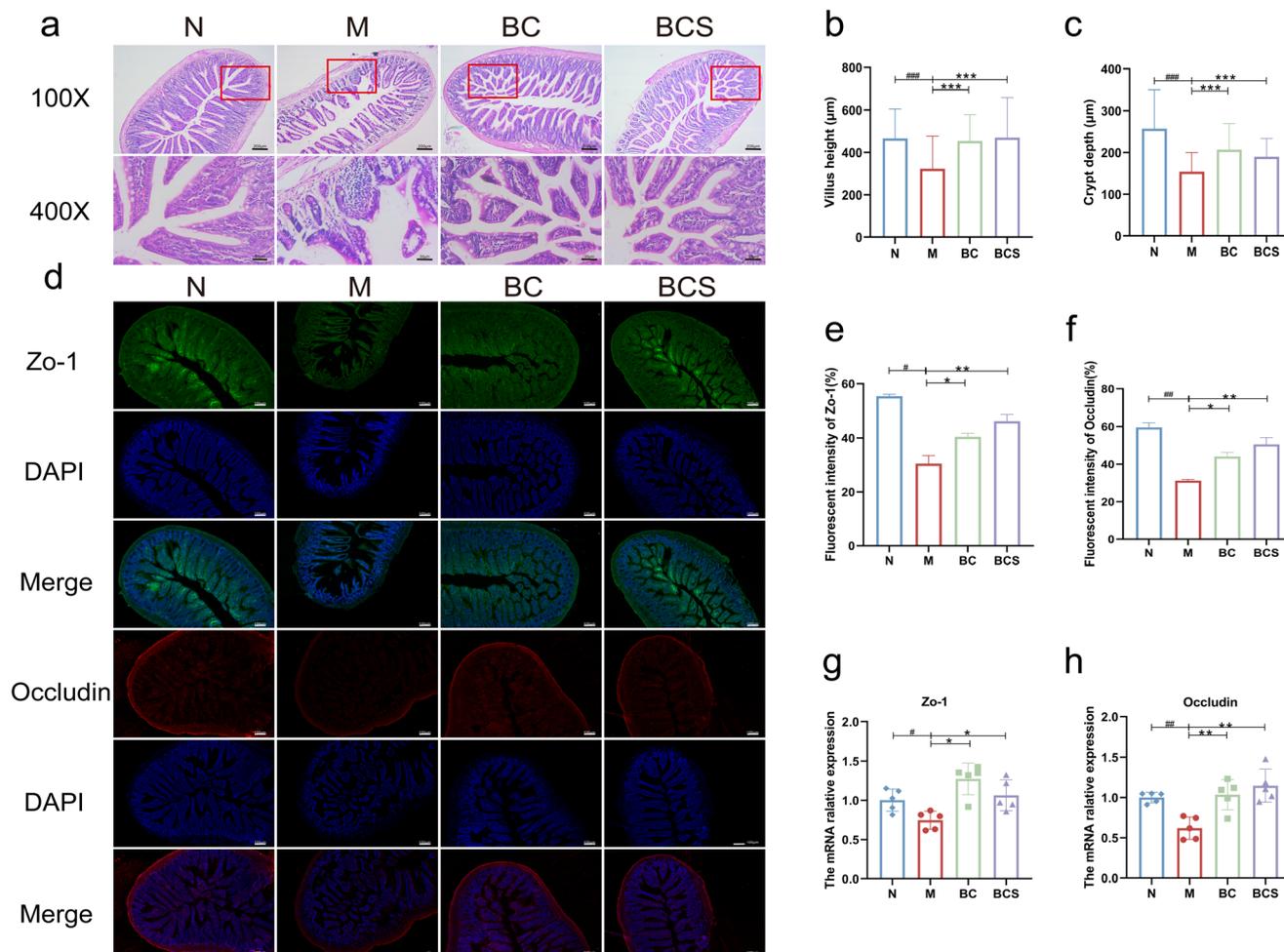
Fig. 4 Effect of *W. coagulans* BCG44 and its supernatant on the intestinal barrier in CTX-induced immunosuppressed mice. (a) Morphologic analysis of the ileum by H&E staining (100× and 400×) ($n = 5$), (b) villus height (μm), (c) crypt depth (μm), (d) immunofluorescence for ZO-1 and occludin protein in ileum tissue (100×). (e) Fluorescence intensity of ZO-1 (%), (f) fluorescence intensity of occludin (%), and (g and h) the mRNA relative expression level of ZO-1 and occludin in the ileum as analysed using RT-qPCR.

abundance of *Acholeplamataceae* was significantly lower in both BC and BCS groups ($P < 0.05$) (Fig. 5b and Fig. S5f†). Moreover, the relative abundance of *Rikenellaceae* and *Akkermansiaceae* was significantly higher in the M group, but the relative abundance of *Rikenellaceae* and *Marinifiaceae* in the BC and BCS groups notably decreased compared to the M group ($P < 0.05$; Fig. 5b and Fig. S5f†). The *Akkermansiaceae* family showed lower relative abundance in the BCS group compared to the M group, while the BC group had an increased relative abundance of the *Oscillospiraceae* family ($P < 0.05$) (Fig. 5b). Similar trends were observed at the genus level. The relative abundance of *Lactobacillus* and *Bacillus* in the BC and BCS groups was significantly increased compared to the N and M groups ($P < 0.05$). Conversely, the relative abundance of *Anaeroplasma* was significantly decreased ($P < 0.05$) in these groups (Fig. 5c and Fig. S5g†). In addition, the relative abundance of *Lachnochlostrium* and *Lachnospiraceae_UCG_006* in the *W. coagulans* BCG44 and its supernatant was higher ($P < 0.05$). Conversely, the relative abundance of *Odoribacter* and

Eubacterium_xylanophilum_group was reduced ($P < 0.05$; Fig. 5c and Fig. S5g†). Specifically, the relative abundance of *Roseburia* in the BCS group was obviously higher than that the M group ($P < 0.05$) (Fig. S5g†).

The alterations of *W. coagulans* BCG44 and its supernatant on gut microbiota biomarkers in CTX-induced immunosuppressed mice

To gain a deeper understanding of the impact of the different groups, we conducted linear discriminant analysis (LEfSe) and generated corresponding linear discriminant analysis (LDA) scores. A screening criterion was set at an LDA value greater than 2.0 to determine the abundance of microorganisms within each group. Our findings revealed that these bacteria were also identified by LEfSe as characteristic microbial communities specific to each group. Notably, *Eubacterium_brachy__group* and *Rikenella* exhibited significant associations with the N group, while *Actinobacteriota*, *Marinifilaceae*, *Odoribacter*, *Devosia*, and *Akkermansiaceae* represented predominant populations within the
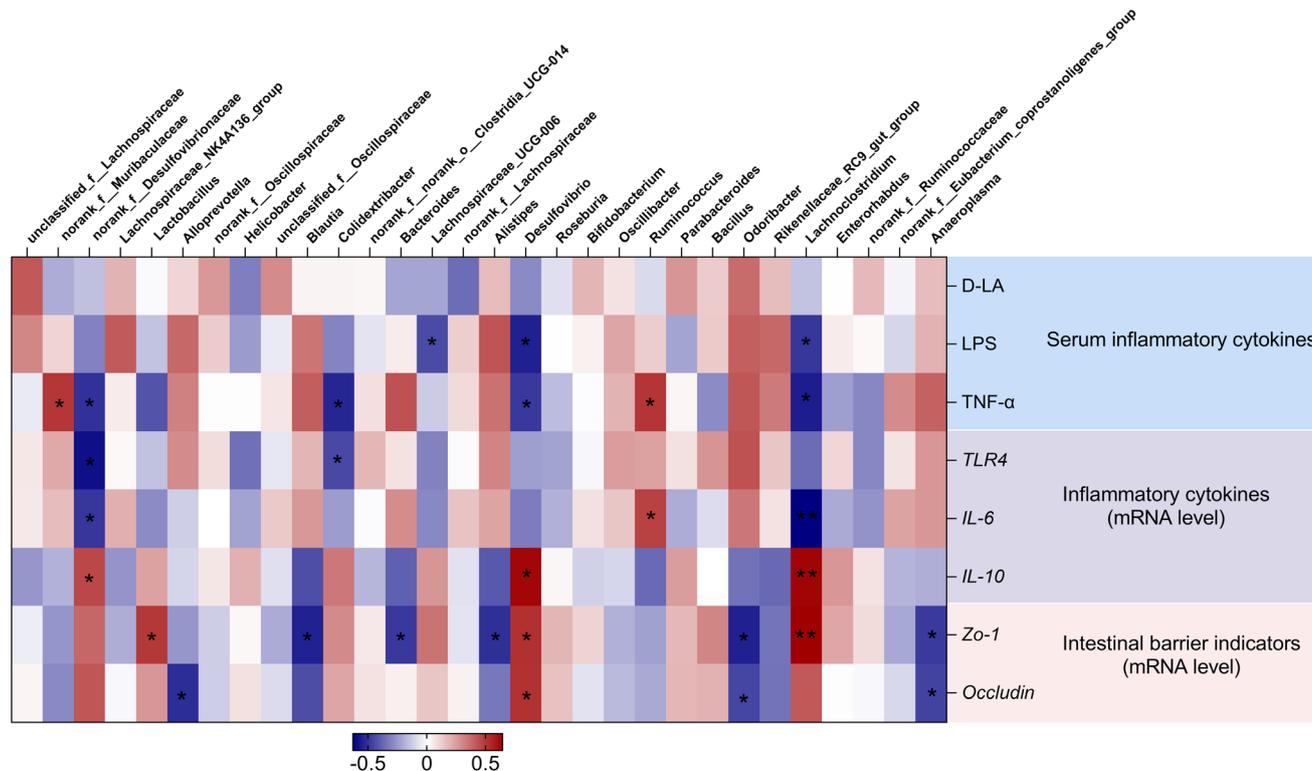
Fig. 5 Effect of *W. coagulans* BCG44 and its supernatant on the gut microbiota in the CTX-induced immunosuppressed mice. (a–c) Microbial distributions of different groups at the phylum, family and genus levels. (d) Principal coordinates analysis (PCoA) with the cluster, (e) nonmetric dimensional scaling (NMDS) with the cluster, and (f) linear discriminate analysis effect size (LEfSe) (LDA score was 2.0) (*n* = 5).

M group. The BC group predominantly consisted of *Bacillaceae* and *Bacillus* species, whereas *Lactobacillaceae* and *Lactobacillus* played vital roles as biomarkers in the BCS group (Fig. 5g).

Correlation between gut microbiota and immunity-related indicators

To investigate the correlation between the gut bacteria and immune indicators, we computed Spearman's correlation coefficient at both the family and genus taxonomic levels (Fig. 6 and Fig. S6†). In the correlation heatmap, at the family level, *Akkermansiaceae* was notably associated with a positive correlation with serum inflammatory cytokines (D-LA, LPS, and TNF-α) and the ileac inflammatory gene expressions (TLR4 and IL-6),

whereas it was negatively correlated with the ileac genes expressions levels (TJ proteins and inflammatory cytokines). *Marinifialceae* positively correlated with the serum inflammatory levels of D-LA and TNF-α (*P* < 0.05), whereas *Rikenellaceae* negatively correlated with the serum TNF-α level (*P* < 0.05). At the genus level, *Lachnoclostridium* showed a negative correlation with LPS, TNF-α and IL-6, but positively correlated with the expression of IL-10 and ZO-1. *Lactobacillus* positively correlated with the ileac mRNA expression of ZO-1, while being negatively correlated with TNF-α. *Lachnospiraceae__UCG_006* was negatively correlated with serum LPS level (*P* < 0.05), and *Anaeroplasma* was negatively correlated with the gut barrier genes expressions of ZO-1 and occludin. *Ruminococcus* displayed a positive correlation with the

Fig. 6 Correlation between intestinal bacteria and immunity-related indicators (n = 5).

serum TNF-α level and the gene expression of IL-6 in the ileum (P < 0.05).

W. coagulans BCG44 and its supernatant changed the function prediction analysis of the gut microbiota and the identification of co-abundance networks

The interactions between the top 50 bacterial species at the genus level are determined using Spearman correlation coefficients, and visualized as a heatmap and correlation network diagram. As shown in Fig. 7a and b, there were two clusters: one was that of *Lactobacillus*, which was negatively correlated with *Oscillibacter* and *Odoribactor* (P < 0.05), while positively correlated with *Bacillus*, unclassified_c__Bacilli, *Bifidobacterium*, and *Faecalibacterium* (P < 0.05). *Anaeroplasma* was negatively correlated with *Bacillus*, unclassified_c__Bacilli, unclassified_f__Oscillospiraceae and norank_f__norank_o__Clostridia_UCG-014 (P < 0.05). Additionally, unclaasified_f__Lachnospiraceae was positively correlated with *Acetatifactor* and A2, *Roseburia* (P < 0.05), whereas *Enterorhabdus* displayed a negative correlation with unclassified_f__Lachnospiraceae and *Acetalifactor* (P < 0.05). We also employed co-occurrence network analyses at the ASV level to examine the dominant species by significant differences in network modules (Fig. 7c and Table S4†). The analysis highlighted unclassified_f__Lachnospiraceae and *Lactobacillus* as highly central members of the gut microbiome, reaching a high hub level. Considering the preceding results, *Lachnospiraceae* and *Lactobacillus* emerged as keystone species[38,40] with substantial

ecological significance. Numerous studies have substantiated the strong link between the immune suppression induced by CTX and the gut microbiota. Consequently, we conducted a comparison of Kyoto Encyclopedia of Genes and Genomes (KEGG) pathways across the groups using Phylogenetic Investigation of Communities by Reconstruction of Unobserved States (PICRUSt) 2 analysis. This approach allowed us to predict and annotate the functions of the gut microbiota. The analysis of level 2 KEGG pathways revealed a significant increase in carbohydrate metabolism, cancer: overview, endocrine system and excretory system in the M group compared with the N group. In contrast, the BC group showed an up-regulation in amino acid metabolism, while the BCS group exhibited a down-regulation in three pathways (drug resistance: antineoplastic, cell growth and death and transport and catabolism). Notably, in the level 3 KEGG pathways, CTX enrichment was observed in seven pathways (the African trypanosomiasis, chagas disease (American trypanosomiasis), pertussis, *Staphylococcus aureus* infection, legionellosis, central carbon metabolism in cancer, renal cell carcinoma, antimicrobial resistance, microRNAs in cancer, and Platelet activation). On the contrary, *W. coagulans* BCG44 and its supernatant reversed the pathway of American trypanosomia compared with the M group. In particular, *W. coagulans* BCG44 supernatant decreased the pathway of MAPK signaling pathway-fly compared with the M group (P < 0.05; Fig. 8 and Fig. S7b, d†).

We further assessed aerobic, anaerobic, contains_mobile_ elements, forms_biofilms, gram_negative, gram_positive, potentially_pathogenic, and stress_tolerant to predict func-
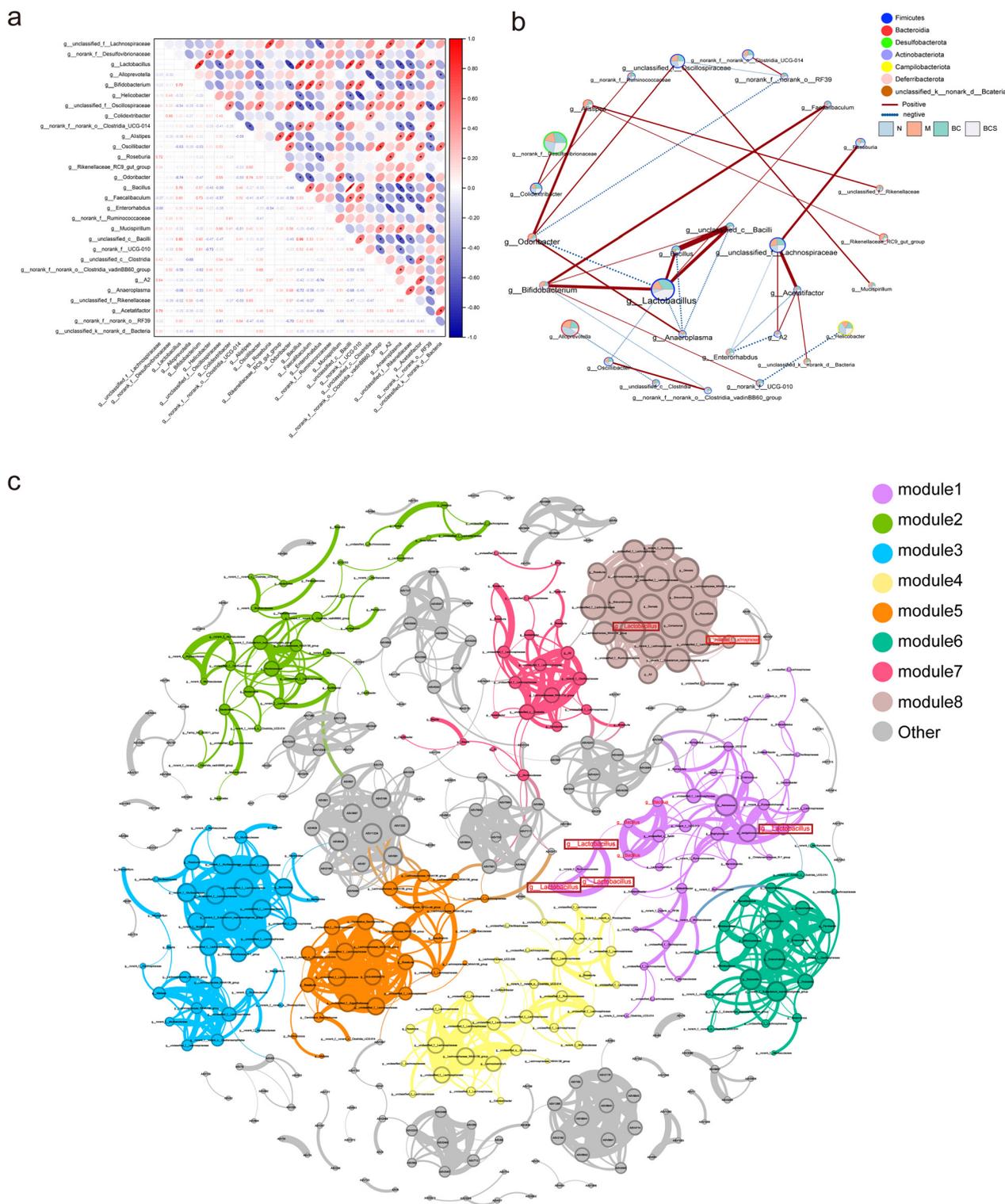
Fig. 7 Network analysis of the intestinal microbiota. (a) Correlation of the top 50 bacteria with relative abundance at the genus level. (b) Single-factor correlation network diagram at the genus level, and (c) co-abundance networks.

tional pathways and biologically interpretable phenotypes (Fig. 8b). The Gram-positive, stress-tolerant, and potentially_-pathogenic in the M group were significantly increased compared with those of the N group ($P < 0.05$). Compared with the

M group, the stress_tolerant and potential_pathogenic of the BC and BCS groups significantly decreased. Compared with the M group, the aerobic, anaerobic and forming_biofilms increased modestly in the BCS group ($P < 0.05$; Fig. 8b).
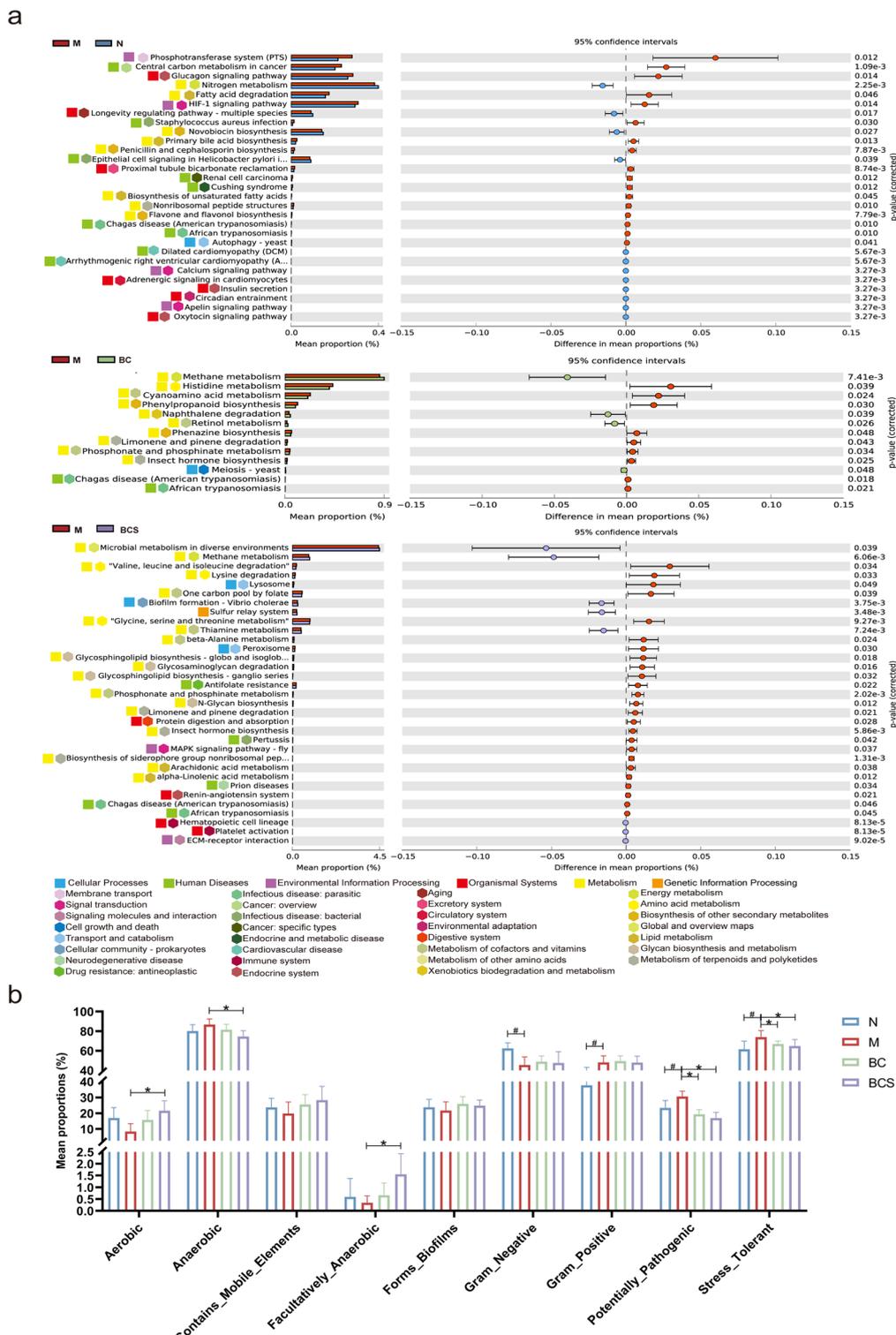
Fig. 8 Effects of *W. coagulans* BCG44 and its supernatant on the metabolic pathways in the gut microbiota based on the Kyoto Encyclopedia of Genes and Genomes (KEGG) database and BugBase analysis. (a) STAMP analysis for the inferred level 3 metabolic pathways, and (b) gut microbiota phenotype (aerobic, anaerobic, contains_mobile_elements, facultatively_ananerobic, forms_biofilms, gram_negative, gram_positive, potentially_-pathogenic, and stress_tolerant).

The effect of the *W. coagulans* BCG44 supernatant on RAW246.7 cells in inflammation and proliferation ability

We detected the viability of RAW264.7 cells exposed to different concentrations (0, 4, 8, 16, and 32 μM) of CTX. Compared with the normal group, the cell viability of cells exposed to CTX (8 μM and 32 μM) was significantly decreased ($P < 0.05$) (Fig. 9a). Ai *et al.* used 10 μM CTX to co-culture the cells;[39] therefore, the following experiments used 8 μM CTX to co-culture with the supernatant of *W. coagulans* BCG44 (1 : 80, 1 : 40 and 1 : 20) (Fig. 9b). When co-cultured with the BCS (1 : 80 and 1 : 40) groups under normal culture conditions, the gene expression levels of IL-10, IL-6 and TLR4 also increased significantly compared with the control group after stimulating the RAW246.7 cells for 24 h ($P < 0.05$) (Fig. 9d–f). In contrast to the 1 : 80 diluted supernatant, TLR4 gene expression in the 1 : 40 diluted supernatant was significantly decreased ($P < 0.05$) (Fig. 9e). Under the culture state of CTX-induced inflammation, the BCS (1 : 80 and 1 : 40) groups significantly increased the cell viability, significantly increased the gene expression levels of IL-10 and IL-6, and decreased the TLR4 mRNA level compared with the CTX group ($P < 0.01$, Fig. 9b and d–f). The IL-10 and IL-6 expression in the 1 : 40 diluted supernatant was significantly up-regulated in contrast to the 1 : 80 diluted supernatant co-cultured with RAW246.7 cells under inflammation ($P < 0.01$). We further used the CCK-8 assay to show that the OD value of the 1 : 40 BCS group after 24 h of culture did not change significantly compared with the control group. After 48 hours, the OD value of the BCS (1 : 40) intervention group was significantly higher than that of the control group ($P < 0.01$, Fig. 9c).

Bioactive metabolites of the cell-free supernatant in *W. coagulans* BCG44

Non-target metabolites of the *W. coagulans* BCG44 supernatant are shown in Table S5.† A variety of metabolites were found, showing a wide range of detected components, including amino acids, carbohydrates, organic compounds, nucleosides and nucleotides. A total of 686 metabolites were detected in positive ion mode, including arginine, C17-sphinganine, L-arginine, *N*-(1-amino-3,3-dimethyl-1-oxobutan-2-yl)-1-pentyl-1*H*-indole-3-carbox, methyl (1-(cyclohexylmethyl)-1*H*-indole-3-carbonyl)-L-valinate, DL-arginine, tyrosine, solamargine, pyridoxine, creatinine, creatine, phe-asn-arg, and leukotriene f4. A total of 516 metabolites were detected in negative ion mode, including tryptophan, DL-lactate, D-mannose, phenyllactic acid, arachidonic acid (peroxide), leucine, thymine, L-leucine, 2-*cis*-4-*trans*-abscisic acid, and telmisartan. In both modes, the top five in the superclass are organic acids and derivatives, lipids and lipid-like molecules, organoheterocyclic compounds, organic nitrogen compounds, and benzenoids (Fig. S6†).

Discussion

There is accumulating reported evidence that CTX suppressed immune function, while also inducing dysbiosis in the gut

microbiota and damaging the intestinal barrier.[41] Probiotic microorganisms have been proven to have beneficial effects on human gut microbiota by inducing the growth of specific genera,[42] and adhering to intestinal epithelial cells to regulate immune responses. As one of the commonly used probiotics in recent years, *B. coagulans* possesses high stability in the gastrointestinal tract, non-toxic action, as well as strong but not yet fully understood pharmacological activity.[43] One way in which bacteria modulate the immune response is its metabolites with the secretion of certain bioactive compounds. Studies have illustrated that metabolites secreted by *B. coagulans* enhance innate immune responses and anti-inflammatory effects *in vitro*.[15]

The *B. coagulans* GBI-30, 6086 strains have been shown to support the maturation of antigen-presenting immune cells, and regulate inflammatory processes in the intestine by reducing pro-inflammatory cytokines. This effect is attributed to its cell wall and metabolite components.[44,45] We found that with or without CTX intervention, the *W. coagulans* BCG44 supernatant co-cultured with RAW246.7 cells *in vitro* demonstrated immunomodulatory effects *via* promoted RAW246.7 cells viability and anti-inflammatory IL-10, and inhibited the gene expression of TLR4. Similar results were observed with the metabolites of *B. coagulans* JBI-YZ6.3 having direct immune activation on RAW264.7 cells in the absence of stimulation.[15] This also promoted the gene expression of IL-6 after the supernatant treatment. As a proinflammatory factor, IL-6 is well-documented to accelerate the spread of inflammation *in vivo*.[46] However, IL-6 also contributes to tissue repair and immune tolerance.[47] IL-6 and IL-10 have previously been shown to enhance the IL-4-dependent induction of the M2 phenotype of macrophages.[48–50] In the presence or absence of disease, the *W. coagulans* BCG44 supernatant may enhance the immune response by assisting macrophages to transform into M2 macrophages with high concentrations of IL-10 and low levels of TLR4.

Consistent with previous observations,[24] our study showed that not only body weight and the spleen index, but also the serum levels of TNF-α were significantly increased in the M group. *W. coagulans* BCG44 and its supernatant normalized the inflammatory levels of TNF-α with the previous reports.[16,51] Moreover, the spleens in the M group exhibited severe damage, confirming that CTX disrupted immune homeostasis, leading to immunosuppression. CTX can directly or indirectly increase the pool of Th17 cells in cancer-bearing hosts.[52] Others have shown that different subsets of CD4$^+$ T cells undergo brief depletion after CTX, including Th1 and Treg cells, and CTX increases the frequency of pathogenic Th17 cells in the spleen.[52,53] Our study validated these findings, showing that *W. coagulans* BCG44 and its supernatant reversed the increase in Th17 proportion and the decrease in Treg proportion. Treg cells play a crucial role in improving the inflammatory response by secreting anti-inflammatory cytokines IL-10, which inhibits self-inflammatory reactions, thereby preventing pathological immune responses that lead to tissue damage.[54,55] The *W. coagulans* BCG44 and its super-
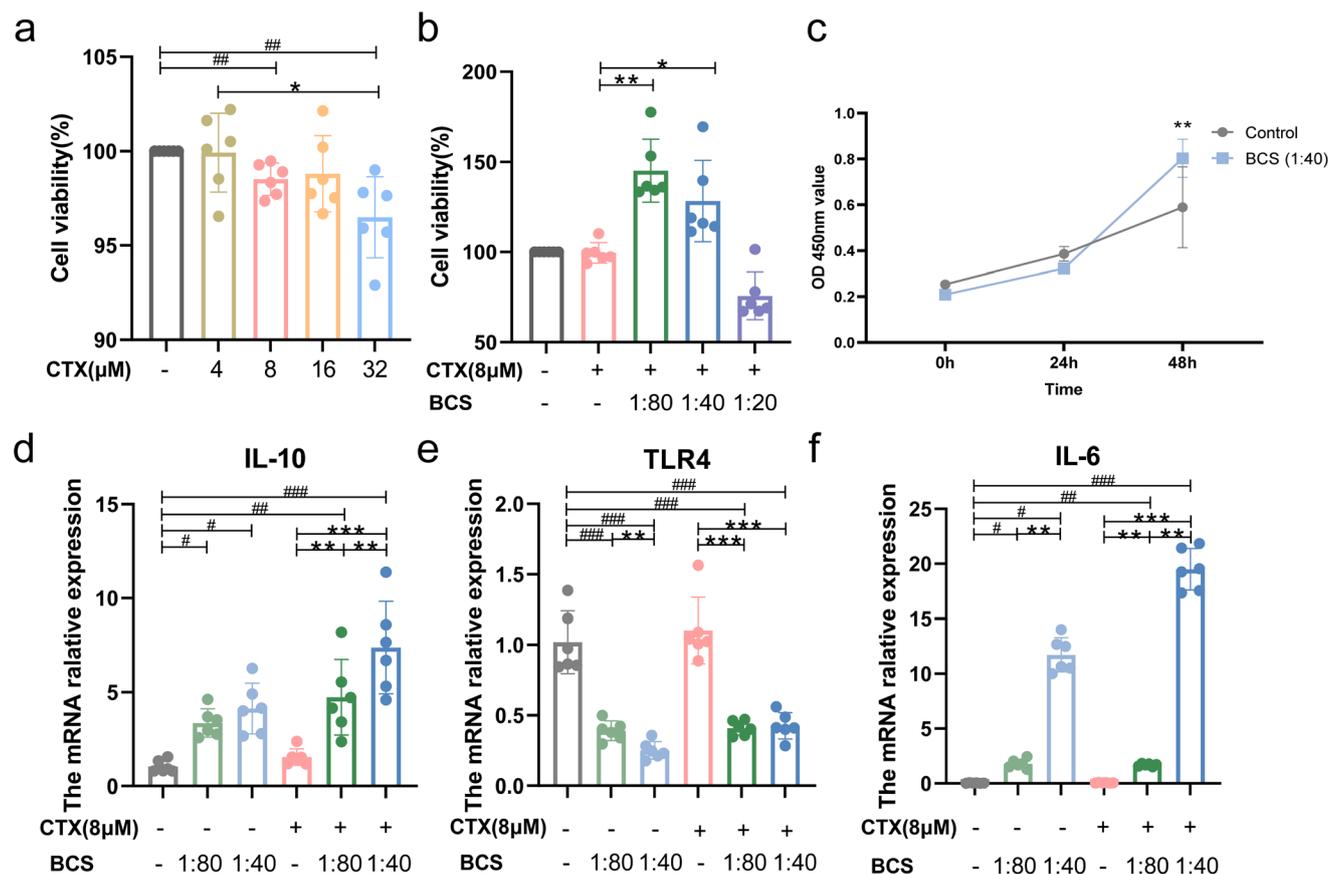
Fig. 9 Effect of the *W. coagulans* BCG44 supernatant on RAW246.7 cells under normal *versus* inflamed culture conditions. (a) Viability of RAW264.7 cells co-cultured with different concentrations of CTX (0, 4, 8, 16 and 32 μM). (b) (b) Viability of RAW264.7cells co-cultured with the concentration of *W.coagulans* BCG44" supernatant (1 : 80, 1 : 40 and 1 : 20) under the intervention of CTX (8 μM). (c) The supernatant (1 : 40) results at 0-, 24-, and 48 h time intervals without the intervention of CTX. (d–f) The mRNA relative expression level of TLR4, IL-6 and IL-10 in the RAW246.7 cells co-cultured with the supernatant (1 : 40 and 1 : 80) under the presence or absence of CTX stimulation using RT-qPCR.

natant up-regulated the ileac mRNA levels of IL-10. These results suggested that *W. coagulans* BC-G44 and its supernatant ameliorated the Th17/Treg imbalance, and resisted inflammatory cytokine levels (TNF-α) in the CTX-induced immune dysfunction.

The intestinal tract is an important mucosal barrier of the body, in which TJ proteins (ZO-1, occludin and Claudin-1) play a defensive role against pathogenic microorganisms.[56,57] The CTX-induced immunosuppressive mice showed abnormalities in the ileum and colon epithelium, accompanied by abnormal inflammatory infiltration and edema patterns. In contrast, the administration of *W. coagulans* BCG44 and its supernatant resulted in reduced inflammatory infiltration and no significant congestion of the intestinal epithelium, with occasional congestion observed, indicating a shift toward normalcy. The goblet cells on the surface of the mucosa can produce mucus, which is the main barrier that restricts contact between the host and symbiotic bacteria and prevents microbial translocation.[58] Genes related to mucus production and tight junction protein expression play a crucial role in intestinal-associated infections.[57] Meanwhile, AB-PAS staining indicated changes in

the intestine. An increase in intestinal mucosal permeability was indicated by elevated levels of serum D-LA and LPS,[59] which was also observed in our results. *W. coagulans* BCG44 and its supernatant decreased the serum levels of LPS, and increased the expression of occludin and ZO-1. The *W. coagulans* BCG44 supernatant decreased the serum levels of D-LA. Increasing evidence suggests that TLR4 activation is one of the important factors in intestinal leakage caused by LPS, therefore leading to the release of inflammatory factors, including TNF-α and IL-6.[60,61] *W. coagulans* BCG44 and its supernatant down-regulated the mRNA levels of (IL-6 and TLR4) of CTX-induced immunosuppressive mice. When mice were stimulated with a high concentration of CTX, the excess production of IL-6 caused a balance between pro-inflammatory and anti-inflammatory responses. The supernatant could reverse this result, which was different from the results of IL-6 *in vitro*. The supernatant can reduce the concentration of LPS and TNF-γ, and thus reduce the production of IL-6 in mice. The relatively high IL-6 concentration observed after RAW264.7 cells are co-cultured with the supernatant may co-promote the polarization of macrophages into M2 macrophages with IL-10.

Together, this suggested that *W. coagulans* BCG44 and its supernatant prevented CTX damage to tight junction proteins and goblet cells, thereby protecting the intestinal mucosal barrier.

The gut microbiota is closely related to intestinal mucosal immunity. *W. coagulans* can modulate the dysbiosis of gut microbiota, which is beneficial to the host. Our research indicates that CTX increased MDI and α-diversity, likely causing confusion in the gut microbiota, which is possibly due to an increase in the types of pathogens in the immunosuppressive mice.[37,62] Regarding β-diversity, *W. coagulans* BCG44 and its supernatant demonstrate a restorative effect on the intestinal microbial structure and composition in immunocompromised mice. Interestingly, the change of *W. coagulans* BCG44 and its supernatant was significantly reversed in gut bacteria at the family and genus levels in CTX-induced immunosuppressed mice. *W. coagulans* BCG44 and its supernatant reduced the relative abundance of *Rikenellaceae* and *Marinifiaceae* at the family level and *Odoribacter* at the genus level. A high relative abundance of *Rikenellaceae* colonized the gut of mice with CTX-induced immunosuppression.[63] *Odoribacter* is associated with the occurrence of colorectal cancer.[64,65] On the contrary, *W. coagulans* BCG44 and its supernatant enriched the relative abundance of some bacteria, including *Lactobacillaceae*, *Lachnospiraceae__UCG-006*, *Lactobacillus*, *Bacillus*, and *Lachnochlostream*, in the CTX-induced mice. Combining multiple results (such as lefse and network analysis), it is important to note that *Lachnospiraceae* and *Lactobacillus* emerged as keystone species with substantial ecological significance. For these bacteria, they have different correlations with the inflammation and intestinal barrier. *Lactobacillus*, known for its probiotic properties, has the ability to alleviate pathogenic infections in the intestinal tract and enhance the host's immune response.[66] Lv *et al.* demonstrated that the combined administration of *Bifidobacterium*, *Lactobacillus*, *Enterococcus*, and *Bacillus* significantly reduced multi-organ damage in immunocompromised rats, and inhibited TLR4 signaling.[28] Bacteria belonging to the *Lachnospiraceae* family are rich members of the healthy human microbiota.[67] Administration of *B. coagulans* SANK 70258 increased bacteria related to the family *Lachnospiraceae*, thereby enhancing butyrate production in the microbiota models of healthy subjects.[68]

Moreover, the supernatant of *W. coagulans* increased the relative abundance of *Roseburia*. *Roseburia* species are known for their ability to penetrate the mucus layer and adhere to the surface of host intestinal epithelial cells, thereby reversing metabolic disturbances and regulating inflammation.[69] The further protective effect of *Roseburia intestinalis* can promote the direct killing of tumor cells on colorectal tumorigenesis *via* derived butyrate.[70] On the other hand, the supernatant of *W. coagulans* BCG44 reduced the relative abundance of *Akkermansiaceae*. *Akkermansiaceae* was found to be positively correlated with immune-inflammatory factors, but negatively correlated with anti-inflammatory factors and tight junction proteins. *Akkermansia* spp., a member of *Akkermansiaceae*, has been shown to enhance the integrity of the epithelial cell layer.

However, in cases of gut microbiota imbalance, *Akkermansia* proliferation and interaction with other microbiota may lead to damage to the intestinal mucus layer.[71,72] Collectively, CTX induced the dysbiosis of gut microbiota, while *W. coagulans* BCG44 and its supernatant restored the imbalance of the microbial ecology *via* regulation of the microbial community structure and composition. This may indicate that *W. coagulans* and its metabolites mainly restore the body's immune function and gut microbiota by affecting the keystone species (*Lachnospirillaceae* and *Lactobacillus*).

Based on a predictive analysis using PICRUSt 2, the KEGG analysis demonstrated a significant decrease in several pro-inflammatory pathways, including American trypanosomiasis, in *W. coagulans* BCG44 and its supernatant groups. The supernatant of *W. coagulans* BCG44 supernatant down-regulated the MAPK signaling pathway in fly. BugBase analysis, which predicts bacterial composition, further indicated that both *W. coagulans* BCG44 and its supernatant restored the potentially_pathogenic and stress_tolerant phenotypes in CTX-induced mice to levels observed in the N group.

Given the immune-enhancing effects of the *W. coagulans* BCG44 supernatant observed above, we further analyzed the metabolites of the supernatant, such as arginine, L-arginine, DL-arginine, DL-lactate, phenyllactic acid, D-mannose, tryptophan and solamargine. Microbial-derived metabolites, such as short-chain fatty acids, branched-chain amino acids, polyamines, and phenolic and indole compounds, have been shown to mediate mucosal immune regulation, epithelial barrier maintenance, and enteroendocrine regulation.[73] Arginine, L-arginine and DL-arginine, accounting for 12.47% of the metabolites, can shape the composition of intestinal microorganisms and improve the host intestinal mucosal immunity.[74] Gao *et al.* have reported that administration of *B. coagulans* TBC169 affected arginine biosynthesis.[75] There is a link between the increased phenyllactic acid content and increased IL-4 and IL-10 production by helper T cells, and the subsequent increase in the effector B cell population.[76] D-Mannose interferes with the normal intracellular metabolism of glucose, thereby slowing the growth of cancer cells.[77] D-Mannose can induce naive T cells in humans and mice to differentiate into Treg, increase the proportion of Treg cells, and inhibit autoimmune diseases and respiratory inflammation.[78] Tryptophan and its metabolites can promote the expression of tight junction proteins in intestinal epithelial cells, inhibit the inflammatory response of macrophages, and regulate the expression of inflammation-related factors.[79] Solamargine has been validated for its multifaceted anti-tumor mechanism, inhibiting the proliferation of cancer cells and effectively inducing apoptosis and autophagy *in vitro* and *in vivo*.[80]

In summary, both *W. coagulans* BCG44 and its supernatant exert a substantial beneficial effect on ameliorating mucosal damage and inflammation, as well as gut microbiota dysbiosis in CTX-induced immunosuppressive mice. Additionally, the supernatant was associated with the production of IL-10 by promoting the growth of macrophages under normal *versus*

CTX-inflamed culture conditions, and contained arginine, phenyllactic acid, D-mannose, tryptophan and solamargine. Meanwhile, considering the small sample size of the experimental study, there may be errors in the experimental results. Future studies with larger sample sizes are warranted to further elucidate the underlying mechanisms by which specific metabolites of *W. coagulation* regulate intestinal immunity during CTX-induced immunosuppression. Furthermore, more comprehensive investigations are warranted to establish a mechanistic connection between *W. coagulans*-specific metabolites and key gut species (*Lachnospirillaceae* and *Lactobacillus*).

Author contributions

Yafang Xu: Writing–original draft, Methodology. Yi Wang: In vitro research, Data curation. Tao Song: Data analysis. Xiaxia Li: Assisted with the animal study. Haolin Zhou: Formal analysis. Oumarou Zafir Chaibou: Review & editing. Bing Wang: Resources. Huajun Li: Supervision. All authors revised and approved the final version of the manuscript.

Data availability

The data supporting this article have been included as part of the ESI.†

Supplementary video material available in Figshare at the following **https://doi.org/10.6084/m9.figshare.25557384**.

Conflicts of interest

The authors have declared that there is no conflict of interest.

Acknowledgements

References

1 S. C. Bischoff and S. Krämer, Human mast cells, bacteria, and intestinal immunity, *Immunol. Rev.*, 2007, **217**, 329–337.

2 H. Kayama, R. Okumura and K. Takeda, Interaction between the microbiota, epithelia, and immune cells in the intestine, *Annu. Rev. Immunol.*, 2020, **38**, 23–48.

3 A. Emadi, R. J. Jones and R. A. Brodsky, Cyclophosphamide and cancer: golden anniversary, *Nat. Rev. Clin Oncol.*, 2009, **6**, 638–647.

4 L. Ye, X. Zhou, M. S. B. Hudari, Z. Li and J. C. Wu, Highly efficient production of L-lactic acid from xylose by newly isolated *Bacillus coagulans*, C106, *Bioresour. Technol.*, 2013, **132**, 38–44.

5 Y. Yu, S. Mo, M. Shen, Y. Chen, Q. Yu, Z. Li and J. Xie, Sulfated modification enhances the immunomodulatory effect of *Cyclocarya paliurus* polysaccharide on cyclophosphamide-induced immunosuppressed mice through MyD88-dependent MAPK/NF-κB and PI3K-Akt signaling pathways, *Food Res. Int.*, 2021, **150**, 110756.

6 X. Huang, X. Zhang, X. Fei, Z. Chen and C. Yu, Effects of *Faecalibacterium prausnitzii* supernatant on Th17 cell and IL-17A in dextran sulfate sodium-induced ulcerative colitis mice, *Zhongnan Daxue Xuebao, Yixueban*, 2015, **40**, 1320–1326.

7 R. Huang, J. Xie, X. Liu and M. Shen, Sulfated modification enhances the modulatory effect of yam polysaccharide on gut microbiota in cyclophosphamide-treated mice, *Food Res. Int.*, 2021, **145**, 110393.

8 K. Halloran and M. A. Underwood, Probiotic mechanisms of action, *Early Hum. Dev.*, 2019, **135**, 58–65.

9 C. M. Thomas and J. Versalovic, Probiotics-host communication: modulation of signaling pathways in the intestine, *Gut Microbes*, 2010, **1**, 148–163.

10 Y. Mu and Y. Cong, *Bacillus coagulans* and its applications in medicine, *Benefic. Microbes*, 2019, **10**, 679–688.

11 B. Hyronimus, C. Le Marrec, A. H. Sassi and A. Deschamps, Acid and bile tolerance of spore-forming lactic acid bacteria, *Int. J. Food Microbiol.*, 2000, **61**, 193–197.

12 K. Abhari, S. S. Shekarforoush, J. Sajedianfard, S. Hosseinzadeh and S. Nazifi, The effects of probiotic, prebiotic and synbiotic diets containing *Bacillus coagulans* and inulin on rat intestinal microbiota, *Iran. J. Vet. Res.*, 2015, **16**, 267–273.

13 S. Zhao, X. Peng, Q. Y. Zhou, Y. Y. Huang, X. Rao, J. L. Tu, H. Y. Xiao and D. M. Liu, *Bacillus coagulans*, 13002 and fructo-oligosaccharides improve the immunity of mice with immunosuppression induced by cyclophosphamide through modulating intestinal-derived and fecal microbiota, *Food Res. Int.*, 2021, **140**, 109793.

14 Z. Zhao, M. Sun, X. Cui, J. Chen, C. Liu and X. Zhang, *Bacillus coagulans* MZY531 alleviates intestinal mucosal injury in immunosuppressive mice via modulating intestinal barrier, inflammatory response, and gut microbiota, *Sci. Rep.*, 2023, **13**, 11181.

15 I. Iloba, S. V. McGarry, L. Yu, D. Cruickshank and G. S. Jensen, Differential immune-modulating activities of cell walls and secreted metabolites from probiotic *Bacillus coagulans* JBI-YZ6.3 under normal versus inflamed culture conditions, *Microorganisms*, 2023, **11**, 2564.

16 Z. Liu, Z. Jiang, Z. Zhang, T. Liu, Y. Fan, T. Liu and N. Peng, *Bacillus coagulans* in combination with chitooligosaccharides regulates gut microbiota and ameliorates the DSS-induced colitis in mice, *Microbiol. Spectrum*, 2023, **10**, e0064122.

17 R. Kumariya, A. K. Garsa, Y. S. Rajput, S. K. Sood, N. Akhtar and S. Patel, Bacteriocins: classification, synthesis, mechanism of action and resistance development in food spoilage causing bacteria, *Microb. Pathog.*, 2019, **128**, 171–177.

18 J. Li, Y. Li, B. Gao, C. Qin, Y. He, F. Xu, H. Yang and M. Lin, Engineering mechanical microenvironment of macrophage and its biomedical applications, *Nanomedicine*, 2018, **13**, 555–576.

19 Y. Wang, J. Lin, Z. Cheng, T. Wang, J. Chen and M. Long, *Bacillus coagulans* TL3 inhibits LPS-induced caecum damage in rat by regulating the TLR4/MyD88/NF-κB and Nrf2 signal pathways and modulating intestinal microflora, *Oxid. Med. Cell. Longevity*, 2022, **2022**, 5463290.

20 Y. Guo, D. Pan, H. Li, Y. Sun, X. Zeng and B. Yan, Antioxidant and immunomodulatory activity of selenium exopolysaccharide produced by *Lactococcus* lactis subsp. lactis, *Food Chem.*, 2013, **138**, 84–89.

21 M. Majeed, K. Nagabhushanam, S. Natarajan, A. Sivakumar, T. Eshuis-de Ruiter, J. Booij-Veurink, Y. P. de Vries and F. Ali, Evaluation of genetic and phenotypic consistency of *Bacillus coagulans* MTCC 5856: a commercial probiotic strain, *World J. Microbiol. Biotechnol.*, 2016, **32**, 60.

22 Y. M. Chen, Y. Li, X. Wang, Z. L. Wang, J. J. Hou, S. Su, W. L. Zhong, X. Xu, J. Zhang, B. M. Wang and Y. M. Wang, Effect of *Bacillus subtilis*, *Enterococcus faecium*, and *Enterococcus faecalis* supernatants on serotonin transporter expression in cells and tissues, *World J. Gastroenterol.*, 2022, **28**, 532–546.

23 A. K. Gupta and C. Maity, Efficacy and safety of *Bacillus coagulans* LBSC in irritable bowel syndrome: A prospective, interventional, randomized, double-blind, placebo-controlled clinical study, *Medicine*, 2021, **100**, e23641.

24 R. M. Gândara, Y. R. Mahida and C. S. Potten, Regional differences in stem and transit cell proliferation and apoptosis in the terminal ileum and colon of mice after 12 Gy, *Int. J. Radiat. Oncol., Biol., Phys.*, 2012, **82**, e521–e528.

25 A. Nestor-Kalinoski, K. M. Smith-Edwards, K. Meerschaert, J. F. Margiotta, B. Rajwa, B. M. Davis and M. J. Howard, Unique neural circuit connectivity of mouse proximal, middle, and distal colon defines regional colonic motor patterns, *Cell. Mol. Gastroenterol. Hepatol.*, 2022, **13**, 309–337.e3.

26 J. Huang, J. Huang, Y. Li, Y. Wang, F. Wang, X. Qiu, X. Liu and H. Li, Sodium alginate modulates immunity, intestinal mucosal barrier function, and gut microbiota in cyclophosphamide-induced immunosuppressed BALB/c mice, *J. Agric. Food Chem.*, 2021, **69**, 7064–7073.

27 J. Huang, H. Zhou, T. Song, B. Wang, H. Ge, D. Zhang, P. Shen, X. Qiu and H. Li, Fecal microbiota transplantation from sodium alginate-dosed mice and normal mice mitigates intestinal barrier injury and gut dysbiosis induced by antibiotics and cyclophosphamide, *Food Funct.*, 2023, **14**, 5690–5701.

28 L. Lv, D. Mu, Y. Du, R. Yan and H. Jiang, Mechanism of the immunomodulatory effect of the combination of live *Bifidobacterium*, *Lactobacillus*, *Enterococcus*, and *Bacillus* on immunocompromised rats, *Front. Immunol.*, 2021, **12**, 694344.

29 X. Zhang, R. Zhang, B. Yu, L. Zhang, H. Chen, Z. Wei, R. Ying, J. Ye, W. Yuan and J. Bai, Protecting effects of a large dose of dexamethasone on spleen injury of rats with severe acute pancreatitis, *J. Gastroenterol. Hepatol.*, 2010, **25**, 302–308.

30 L. Wang, F. Zhu, H. Yang, J. Li, Y. Li, X. Ding, X. Xiong and Y. Yin, Effects of dietary supplementation with epidermal growth factor on nutrient digestibility, intestinal development and expression of nutrient transporters in early-weaned piglets, *J. Anim. Physiol. Anim. Nutr.*, 2019, **103**, 618–625.

31 M. Wang, C. Yang, Q. Wang, J. Li, P. Huang, Y. Li, X. Ding, H. Yang and Y. Yin, The relationship between villous height and growth performance, small intestinal mucosal enzymes activities and nutrient transporters expression in weaned piglets, *J. Anim. Physiol. Anim. Nutr.*, 2020, **104**, 606–615.

32 D. Chang, C. F. Kim, M. Horton, D. Lee, M. C. Pacheco, J. A. Silvester and J. D. Goldsmith, A tip-predominant distribution of villous intraepithelial lymphocytes is not specific to celiac disease in children with Marsh I lesions, *Am. J. Clin. Pathol.*, 2024, **161**, 149–154.

33 L. Liu, D. Chen, B. Yu, H. Yin, Z. Huang, Y. Luo, P. Zheng, X. Mao, J. Yu, J. Luo, H. Yan and J. He, Fructooligosaccharides improve growth performance and intestinal epithelium function in weaned pigs exposed to enterotoxigenic *Escherichia coli*, *Food Funct.*, 2020, **11**, 9599–9612.

34 M. Guo, H. Liu, Y. Yu, X. Zhu, H. Xie, C. Wei, C. Mei, Y. Shi, N. Zhou, K. Qin and W. Li, *Lactobacillus rhamnosus* GG ameliorates osteoporosis in ovariectomized rats by regulating the Th17/Treg balance and gut microbiota structure, *Gut Microbes*, 2023, **15**, 2190304.

35 R. D. Specian and M. R. Neutra, Regulation of intestinal goblet cell secretion. I. role of parasympathetic stimulation, *Am. J. Physiol.*, 1982, **242**, G370–G379.

36 D. Chrysostomou, L. A. Roberts, J. R. Marchesi and J. M. Kinross, Gut microbiota modulation of efficacy and toxicity of cancer chemotherapy and immunotherapy, *Gastroenterology*, 2023, **164**, 198–213.

37 F. Li, M. Wang, J. Wang, R. Li and Y. Zhang, Alterations to the gut microbiota and their correlation with inflammatory factors in chronic kidney disease, *Front. Cell. Infect. Microbiol.*, 2019, **9**, 206.

38 Y. Kang, X. Kang, H. Yang, H. Liu, X. Yang, Q. Liu, H. Tian, Y. Xue, P. Ren, X. Kuang, Y. Cai, M. Tong, L. Li and W. Fan, *Lactobacillus acidophilus* ameliorates obesity in mice through modulation of gut microbiota dysbiosis and intestinal permeability, *Pharmacol. Res.*, 2022, **175**, 106020.

39 G. Ai, M. Meng, J. Guo, C. Li, J. Zhu, L. Liu, B. Liu, W. Yang, X. Shao, Z. Cheng and L. Wang, Adipose-derived stem cells promote the repair of chemotherapy-induced premature ovarian failure by inhibiting granulosa cells apoptosis and senescence, *Stem Cell Res. Ther.*, 2023, **14**, 75.

40 S. Banerjee, K. Schlaeppi and M. G. A. van der Heijden, Keystone taxa as drivers of microbiome structure and functioning, *Nat. Rev. Microbiol.*, 2018, **16**, 567–576.

41 R. Daillère, M. Vétizou, N. Waldschmitt, T. Yamazaki, C. Isnard, V. Poirier-Colame, C. P. M. Duong, C. Flament, P. Lepage, M. P. Roberti, B. Routy, N. Jacquelot, L. Apetoh, S. Becharef, S. Rusakiewicz, P. Langella, H. Sokol, G. Kroemer, D. Enot, A. Roux, A. Eggermont, E. Tartour, L. Johannes, P. L. Woerther, E. Chachaty, J. C. Soria, E. Golden, S. Formenti, M. Plebanski, M. Madondo, P. Rosenstiel, D. Raoult, V. Cattoir, I. G. Boneca, M. Chamaillard and L. Zitvogel, *Enterococcus hirae* and *Barnesiella intestinihominis* facilitate cyclophosphamide-induced therapeutic immunomodulatory effects, *Immunity*, 2016, **45**, 931–943.

42 A. Szydłowska and B. Sionek, Probiotics and postbiotics as the functional food components affecting the immune response, *Microorganisms*, 2022, **11**, 104.

43 N. K. Lee, W. S. Kim and H. D. Paik, *Bacillus* strains as human probiotics: characterization, safety, microbiome, and probiotic carrier, *Food Sci. Biotechnol.*, 2019, **28**, 1297–1305.

44 G. S. Jensen, K. F. Benson, S. G. Carter and J. R. Endres, GanedenBC30TM cell wall and metabolites: anti-inflammatory and immune modulating effects in vitro, *BMC Immunol.*, 2010, **11**, 15.

45 K. F. Benson, K. A. Redman, S. G. Carter, D. Keller, S. Farmer, J. R. Endres and G. S. Jensen, Probiotic metabolites from *Bacillus coagulans* GanedenBC30TM support maturation of antigen-presenting cells in vitro, *World J. Gastroenterol.*, 2012, **18**, 1875–1883.

46 J. Scheller, A. Chalaris, D. Schmidt-Arras and S. Rose-John, The pro- and anti-inflammatory properties of the cytokine interleukin-6, *Biochim. Biophys. Acta*, 2011, **1813**, 878–888.

47 D. E. Johnson, R. A. O'Keefe and J. R. Grandis, Targeting the IL-6/JAK/STAT3 signalling axis in cancer, *Nat. Rev. Clin Oncol.*, 2018, **15**, 234–248.

48 J. Mauer, B. Chaurasia, J. Goldau, M. C. Vogt, J. Ruud, K. D. Nguyen, S. Theurich, A. C. Hausen, J. Schmitz, H. S. Brönneke, E. Estevez, T. L. Allen, A. Mesaros, L. Partridge, M. A. Febbraio, A. Chawla, F. T. Wunderlich and J. C. Brüning, Signaling by IL-6 promotes alternative activation of macrophages to limit endotoxemia and obesity-associated resistance to insulin, *Nat. Immunol.*, 2014, **15**, 423–430.

49 N. Makita, Y. Hizukuri, K. Yamashiro, M. Murakawa and Y. Hayashi, IL-10 enhances the phenotype of M2 macrophages induced by IL-4 and confers the ability to increase eosinophil migration, *Int. Immunol.*, 2015, **27**, 131–141.

50 M. R. Fernando, J. L. Reyes, J. Iannuzzi, G. Leung and D. M. McKay, The pro-inflammatory cytokine, interleukin-6, enhances the polarization of alternatively activated macrophages, *PLoS One*, 2014, **9**, e94188.

51 T. V. Bomko, T. N. Nosalskaya, T. V. Kabluchko, Y. V. Lisnyak and A. V. Martynov, Immunotropic aspect of the *Bacillus coagulans* probiotic action, *J. Pharm. Pharmacol.*, 2017, **69**, 1033–1040.

52 S. Viaud, C. Flament, M. Zoubir, P. Pautier, A. LeCesne, V. Ribrag, J.-C. Soria, V. Marty, P. Vielh, C. Robert, N. Chaput and L. Zitvogel, Cyclophosphamide induces differentiation of Th17 cells in cancer patients, *Cancer Res.*, 2011, **71**, 661–665.

53 C. Buccione, A. Fragale, F. Polverino, G. Ziccheddu, E. Aricò, F. Belardelli, E. Proietti, A. Battistini and F. Moschella, Role of interferon regulatory factor 1 in governing Treg depletion, Th1 polarization, inflammasome activation and antitumor efficacy of cyclophosphamide, *Int. J. Cancer*, 2018, **142**, 976–987.

54 M. F. Neurath, Cytokines in inflammatory bowel disease, *Nat. Rev. Immunol.*, 2014, **14**, 329–342.

55 S. Z. Josefowicz, L. F. Lu and A. Y. Rudensky, Regulatory T cells: mechanisms of differentiation and function, *Annu. Rev. Immunol.*, 2012, **30**, 531–564.

56 Y. Wu, L. Tang, B. Wang, Q. Sun, P. Zhao and W. Li, The role of autophagy in maintaining intestinal mucosal barrier, *J. Cell Physiol.*, 2019, **234**, 19406–19419.

57 M. Furuse, M. Hata, K. Furuse, Y. Yoshida, A. Haratake, Y. Sugitani, T. Noda, A. Kubo and S. Tsukita, Claudin-based tight junctions are crucial for the mammalian epidermal barrier: a lesson from claudin-1-deficient mice, *J. Cell Biol.*, 2002, **156**, 1099–1111.

58 R. D. Specian and M. G. Oliver, Functional biology of intestinal goblet cells, *Am. J. Physiol.*, 1991, **260**, C183–C193.

59 R. Zhu, L. Li, M. Li, Z. Yu, H. H. Wang, Y. N. Quan and L. F. Wu, Effects of dietary glycinin on the growth performance, immunity, hepatopancreas and intestinal health of juvenile Rhynchocypris lagowskii Dybowski, *Aquaculture*, 2021, **544**, 737030.

60 R. J. Xavier and D. K. Podolsky, Unravelling the pathogenesis of inflammatory bowel disease, *Nature*, 2007, **448**, 427–434.

61 Y. C. Lu, W. C. Yeh and P. S. Ohashi, LPS/TLR4 signal transduction pathway, *Cytokine*, 2008, **42**, 145–151.

62 D. Yu, X. Yu, A. Ye, C. Xu, X. Li, W. Geng and L. Zhu, Profiling of gut microbial dysbiosis in adults with myeloid leukemia, *FEBS Open Bio*, 2021, **11**, 2050–2059.

63 J. P. Liu, J. Wang, S. X. Zhou, D. C. Huang, G. H. Qi and G. T. Chen, Ginger polysaccharides enhance intestinal immunity by modulating gut microbiota in cyclophosphamide-induced immunosuppressed mice, *Int. J. Biol. Macromol.*, 2022, **223**, 1308–1319.

64 J. P. Zackular, N. T. Baxter, K. D. Iverson, W. D. Sadler, J. F. Petrosino, G. Y. Chen and P. D. Schloss, The gut microbiome modulates colon tumorigenesis, *mBio*, 2013, **4**, e00692-13.

65 P. G. Wolf, V. Kolosslov, Z. Zhou, L. Ly, H. Doden, S. Devendran, A. M. Breister, L. Lucio, P. Polak, S. Matatov, K. Anantharaman, J. M. Ridlon and R. Gaskins, The gut microbiome modulates colon tumorigenesis, Abstract 3342: The colorectal cancer associated microbe *Odoribacter splanchnicus* produces genotoxic hydrogen sulfide via cysteine metabolism, *Cancer Res.*, 2020, **80**, 3342–3342.

66 V. Liévin-Le Moal and A. L. Servin, Anti-infective activities of *lactobacillus* strains in the human intestinal microbiota: from probiotics to gastrointestinal anti-infectious biotherapeutic agents, *Clin. Microbiol. Rev.*, 2014, **27**, 167–199.

67 M. Vacca, G. Celano, F. M. Calabrese, P. Portincasa, M. Gobbetti and M. De Angelis, The controversial role of human gut *Lachnospiraceae*, *Microorganisms*, 2020, **8**, 573.

68 K. Sasaki, D. Sasaki, J. Inoue, N. Hoshi, T. Maeda, R. Yamada and A. Kondo, *Bacillus coagulans* SANK 70258 suppresses *Enterobacteriaceae* in the microbiota of ulcerative colitis in vitro and enhances butyrogenesis in healthy microbiota, *Appl. Microbiol. Biotechnol.*, 2020, **104**, 3859–3867.

69 P. Van den Abbeele, C. Belzer, M. Goossens, M. Kleerebezem, W. M. De Vos, O. Thas, R. De Weirdt, F.-M. Kerckhof and T. Van de Wiele, Butyrate-producing *Clostridium* cluster XIVa species specifically colonize mucins in an in vitro gut model, *ISME J.*, 2013, **7**, 949–961.

70 X. Kang, C. Liu, Y. Ding, Y. Ni, F. Ji, H. C. H. Lau, L. Jiang, J. J. Sung, S. H. Wong and J. Yu, *Roseburia intestinalis* generated butyrate boosts anti-PD-1 efficacy in colorectal cancer by activating cytotoxic CD8$^+$ T cells, *Gut*, 2023, **72**, 2112–2122.

71 S. Romano, G. M. Savva, J. R. Bedarf, I. G. Charles, F. Hildebrand and A. Narbad, Meta-analysis of the Parkinson's disease gut microbiome suggests alterations linked to intestinal inflammation, *npj Parkinson's Dis.*, 2021, **7**, 27.

72 M. S. Desai, A. M. Seekatz, N. M. Koropatkin, N. Kamada, C. A. Hickey, M. Wolter, N. A. Pudlo, S. Kitamoto, N. Terrapon, A. Muller, V. B. Young, B. Henrissat, P. Wilmes, T. S. Stappenbeck, G. Núñez and E. C. Martens, A dietary fiber-deprived gut microbiota degrades the colonic mucus barrier and enhances pathogen susceptibility, *Cell*, 2016, **167**, 1339–1353.e21.

73 L. Wu, Z. Tang, H. Chen, Z. Ren, Q. Ding, K. Liang and Z. Sun, Mutual interaction between gut microbiota and protein/amino acid metabolism for host mucosal immunity and health, *Anim. Nutr.*, 2021, **7**, 11–16.

74 X. Zheng, B. Liu, N. Wang, J. Yang, Q. Zhou, C. Sun and Y. Zhao, Low fish meal diet supplemented with probiotics ameliorates intestinal barrier and immunological function of *Macrobrachium rosenbergii* via the targeted modulation of gut microbes and derived secondary metabolites, *Front. Immunol.*, 2022, **13**, 1074399.

75 W. Gao, Y. Yan, Z. Guan, J. Zhang and W. Chen, Effects of B*acillus coagulans* TBC169 on gut microbiota and metabolites in gynecological laparoscopy patients, *Front. Microbiol.*, 2024, **15**, 1284402.

76 N. Oezguen, V. Yılmaz, T. D. Horvath, E. Akbayir, S. J. Haidacher, K. M. Hoch, S. Thapa, J. Palacio, R. Türkoğlu, M. Kürtüncü, M. A. Engevik, J. Versalovic, A. M. Haag and E. Tüzün, Serum 3-phenyllactic acid level is reduced in benign multiple sclerosis and is associated with effector B cell ratios, *Mult. Scler. Relat. Disord.*, 2022, **68**, 104239.

77 P. S. Gonzalez, J. O'Prey, S. Cardaci, V. J. A. Barthet, J. I. Sakamaki, F. Beaumatin, A. Roseweir, D. M. Gay, G. Mackay, G. Malviya, E. Kania, S. Ritchie, A. D. Baudot, B. Zunino, A. Mrowinska, C. Nixon, D. Ennis, A. Hoyle, D. Millan, I. A. McNeish, O. J. Sansom, J. Edwards and K. M. Ryan, Mannose impairs tumour growth and enhances chemotherapy, *Nature*, 2018, **563**, 719–723.

78 D. Zhang, C. Chia, X. Jiao, W. Jin, S. Kasagi, R. Wu, J. E. Konkel, H. Nakatsukasa, P. Zanvit, N. Goldberg, Q. Chen, L. Sun, Z. J. Chen and W. Chen, D-mannose induces regulatory T cells and suppresses immunopathology, *Nat. Med.*, 2017, **23**, 1036–1045.

79 C. Xue, G. Li, Q. Zheng, X. Gu, Q. Shi, Y. Su, Q. Chu, X. Yuan, Z. Bao, J. Lu and L. Li, Tryptophan metabolism in health and disease, *Cell Metab.*, 2023, **35**, 1304–1326.

80 S. Yin, W. Jin, Y. Qiu, L. Fu, T. Wang and H. Yu, Solamargine induces hepatocellular carcinoma cell apoptosis and autophagy via inhibiting LIF/miR-192-5p/CYR61/Akt signaling pathways and eliciting immunostimulatory tumor microenvironment, *J. Hematol. Oncol.*, 2022, **15**, 32.